INSTITUTO POLITÉCNICO NACIONAL

CENTRO DE INVESTIGACIÓN EN CIENCIA APLICADA Y TECNOLOGÍA AVANZADA - UNIDAD QUERÉTARO

POSTGRADUATE IN ADVANCED TECHNOLOGY

STRUCTURE AND FUNCTIONALITY OF ACID HYDROLYZED AND AUTOCLAVED CORN STARCHES WITH DIFFERENT AMYLOSE CONTENT

THESIS TO OBTAIN THE DEGREE OF

DOCTOR IN ADVANCED TECHNOLOGY

P R E S E N T E D B Y:

M. ADRIÁN GUADALUPE SOLER MARTÍNEZ

DIRECTED BY:

Dr. MA. GUADALUPE MÉNDEZ MONTEALVO **Dr. GONZALO VELAZQUEZ DE LA CRUZ**

May 2020

SIP-13
REP 2017

INSTITUTO POLITÉCNICO NACIONAL
SECRETARIA DE INVESTIGACIÓN Y POSGRADO

ACTA DE REGISTRO DE TEMA DE TESIS
Y DESIGNACIÓN DE DIRECTOR DE TESIS

Ciudad de México, a 8 de junio de 2020

El Colegio de Profesores de Posgrado de **CICATA Unidad Querétaro** en su Sesión **ordinaria** No. **200605** celebrada el día **5** del mes **junio** de **2020**, conoció la solicitud presentada por el alumno:

Apellido Paterno:	Soler	Apellido Materno:	Martínez	Nombre (s):	Adrián Guadalupe

Número de registro: A 1 6 0 9 8 5

del Programa Académico de Posgrado: Doctorado en Tecnología Avanzada

Referente al registro de su tema de tesis; acordando lo siguiente:

1.- Se designa al aspirante el tema de tesis titulado:

Structure and functionality of acid hydrolyzed and autoclaved corn starches with different amylose content

Objetivo general del trabajo de tesis:

Estudiar el efecto de las modificaciones de almidones de maíz con diferente contenido de amilosa tratados por hidrólisis ácida y autoclave sobre la estructura y las propiedades funcionales.

2.- Se designa como Directores de Tesis a los profesores:

Director: Dra. Ma. Guadalupe del Carmen Méndez Montealvo

2° Director: Dr. Gonzalo Velazquez de la Cruz

No aplica: ☐

3.- El Trabajo de investigación base para el desarrollo de la tesis será elaborado por el alumno en:

CICATA-Unidad Querétaro

que cuenta con los recursos e infraestructura necesarios.

4.- El interesado deberá asistir a los seminarios desarrollados en el área de adscripción del trabajo desde la fecha en que se suscribe la presente, hasta la aprobación de la versión completa de la tesis por parte de la Comisión Revisora correspondiente.

Director de Tesis

Dra. Ma. Guadalupe del Carmen Méndez Montealvo

2° Director de Tesis

Dr. Gonzalo Velazquez de la Cruz

Aspirante

Adrián Guadalupe Soler Martínez

Presidente del Colegio

Dr. Alejandro Alfredo Lozano Guzmán

INSTITUTO POLITÉCNICO NACIONAL
CENTRO DE INVESTIGACIÓN EN CIENCIA APLICADA Y TECNOLOGÍA AVANZADA
UNIDAD QUERÉTARO
DIRECCIÓN

SIP-14
REP 2017

INSTITUTO POLITÉCNICO NACIONAL

SECRETARÍA DE INVESTIGACIÓN Y POSGRADO

ACTA DE REVISIÓN DE TESIS

En la Ciudad de Querétaro siendo las 12:00 horas del día 1 del mes de junio del 2020 se reunieron los miembros de la Comisión Revisora de la Tesis, designada por el Colegio de Profesores de Posgrado de: CICATA-IPN QRO para examinar la tesis titulada:

Structure and functionality of acid hydrolyzed and autoclaved corn starches with different amylose content

del alumno:

Apellido Paterno:	Soler	Apellido Materno:	Martínez	Nombre (s):	Adrián Guadalupe

Número de registro: A 1 6 0 9 8 5

Aspirante del Programa Académico de Posgrado: Doctorado en Tecnología Avanzada

Una vez que se realizó un análisis de similitud de texto, utilizando el software antiplagio, se encontró que el trabajo de tesis tiene un 34 % de similitud. **Se adjunta reporte de software utilizado**.

Después que esta Comisión revisó exhaustivamente el contenido, estructura, intención y ubicación de los textos de la tesis identificados como coincidentes con otros documentos, concluyó que en el presente tra☐o **SI** ☐ **NO** ✓ **SE CONSTITUYE UN POSIBLE PLAGIO.**

JUSTIFICACIÓN DE LA CONCLUSIÓN:

En el análisis de similitud del documento de tesis no se encontraron frases completas idénticas a otras fuentes. Del 34% de similitud, el 21% corresponde a dos de los artículos derivados de este trabajo de tesis. El resto del porcentaje de similitud corresponde a palabras aisladas de uso común en el área.

Es responsabilidad del alumno como autor de la tesis la verificación antiplagio y del Director o Directores de tesis el análisis del % de similitud para establecer el riesgo o la existencia de un posible plagio.

Finalmente y posterior a la lectura, revisión individual, así como el análisis e intercambio de opiniones, los miembros de la Comisión manifestaron **APROBAR** ☑ **SUSPENDER** ☐ **NO APROBAR** ☐ la tesis por **UNANIMIDAD** ☑ o **MAYORÍA** ☐ en virtud de los motivos siguientes:

El trabajo desarrollado, así como la compresión y discusión de la información obtenida se considera que cumplen con los requisitos para proceder a sustentar el examen de grado al cual aspira.

COMISIÓN REVISORA DE TESIS

Director de Tesis
Dra. Ma. Guadalupe del Carmen Méndez Montealvo

Dra. Perla Osorio Díaz (CEPROBI-IPN)

Eduardo Morales S.

Dr. Eduardo Morales Sánchez

2° Director de Tesis
Dr. Gonzalo Velázquez de la Cruz

Dr. Pedro Alberto Vázquez Landaverde

Dr. Alejandro Alfredo Lozano Guzmán
PRESIDENTE DEL COLEGIO DE PROFESORES

SECRETARÍA DE EDUCACIÓN PÚBLICA · PODER EJECUTIVO FEDERAL · ESTADOS UNIDOS MEXICANOS · MÉXICO

INSTITUTO POLITÉCNICO NACIONAL
CENTRO DE INVESTIGACIÓN EN TECNOLOGÍA AVANZADA
UNIDAD QUERÉTARO
DIRECCIÓN

INSTITUTO POLITÉCNICO NACIONAL

SECRETARÍA DE INVESTIGACIÓN Y POSGRADO

CARTA CESIÓN DE DERECHOS

En la Ciudad de **México, D. F.** el día **07** del mes de **mayo** del año **2020**, el que suscribe **Adrián Guadalupe Soler Martínez** alumno del Programa de **Doctorado en Tecnología Avanzada** con número de registro **A160985**, adscrito al **Centro de Investigación en Ciencia Aplicada y Tecnología Avanzada unidad Querétaro**, manifiesta que es autor intelectual del presente trabajo de Tesis bajo la dirección de la **Dra. Ma. Guadalupe del Carmen Méndez Montealvo** y el **Dr. Gonzalo Velazquez de la Cruz** y cede los derechos del trabajo titulado **"Structure and functionality of acid hydrolyzed and autoclaved corn starches with different amylose content"**, al **Instituto Politécnico Nacional** para su difusión, con fines académicos y de investigación.

Los usuarios de la información no deben reproducir el contenido textual, gráficas o datos del trabajo sin el permiso expreso del autor y/o director del trabajo. Este puede ser obtenido escribiendo a la siguiente dirección **cmendez@ipn.mx, gvelazquezd@ipn.mx y agsm84@hotmail.com.** Si el permiso se otorga, el usuario deberá dar el agradecimiento correspondiente y citar la fuente del mismo.

Adrián Guadalupe Soler Martínez

Abstract

Starch is the main source of energy for humans and a suitable biomaterial for industrial applications. The structure of native starches is modified by different methods to enhance its functionality. Acid hydrolysis and autoclaving are modification methods widely used to improve the functional properties of starch. Despite the abundant literature available about the effects of those methods on the structure and functionality of starch, at present, the influence of the structure of the modified starches on the functionality is not fully understood. This study aimed to investigate the effect of both methods on the structure of two corn starches with different amylose content and explain its influence on the functionality. Normal (NS) and high amylose, Hylon VII (HS) corn starches were acid hydrolyzed for 3, 6, 9, 12, and 15 days at 25 °C or autoclaved at 105, 120, and 135 °C for 30 min. Also, the autoclaved starches (ANS and AHS) at 120 °C were retrograded under a range of water contents at 20 °C. The granular morphology and the crystalline and double-helical structure were studied. Also, the solubility, swelling, water/oil holding capacity, and resistance to enzymatic digestion were the functional properties evaluated. The results showed that the acid hydrolysis was the most effective treatment to improve the solubility and oil holding capacity of both starches, due to the high degradative effect induced by the acid on the granules and the formation of appropriate helical structures for the entrapment of the oil, respectively. On the other hand, the autoclaving treatment was more effective to improve the swelling and water holding capacity of both starches, by strengthening the interactions between the molecular components of starch. Such interactions improved the crystallite quality, responsible for the increase of the resistance to the enzymatic digestion in both starches. Moreover, the double-helical order affected the resistance to enzymatic digestion in the modified HS. In the retrograded autoclaved starches, the water molecules plasticized the

starch chains promoting their arrangement in close-packed double helices and crystalline regions. Also, the formation of homogeneous double-helical crystallites of amylose increased the resistance to the enzymatic digestion of retrograded AHS. In ANS, the recrystallization of amylopectin prevented the formation of homogeneous amylose crystallites decreasing the resistance to enzymatic digestion. The selection of the appropriate modification method and process condition allows imparting specific functional properties to NS and HS. The scientific findings of this work can help to design novel modified starches with desired functionality.

Resumen

El almidón es la fuente primaria de energía para los humanos y un biomaterial adecuado para aplicaciones industriales. La estructura de los almidones nativos es modificada por diferentes métodos con el objetivo de aumentar su funcionalidad. La hidrólisis ácida y el tratamiento en autoclave son métodos de modificación ampliamente utilizados para mejorar las propiedades funcionales del almidón. La literatura disponible acerca de los efectos de esos métodos sobre la estructura y la funcionalidad del almidón es abundante; sin embargo, actualmente, la influencia de la estructura de los almidones modificados sobre su funcionalidad no está comprendida completamente. El objetivo de este estudio fue investigar el efecto de ambos métodos sobre la estructura de dos almidones de maíz con diferente contenido de amilosa y explicar su influencia en la funcionalidad. Almidones de maíz normal (NS) y alto en amilosa, Hylon VII (HS) se hidrolizaron con ácido por 3, 6, 9, 12 y 15 días a 25 °C o se trataron en autoclave a 105, 120 y 135 °C por 30 min. Además, los almidones tratados en autoclave (ANS y AHS) a 120 °C se retrogradaron bajo diferentes contenidos de agua a 20 °C. Se estudió la morfología granular y la estructura cristalina y de dobles hélices y se evaluaron las propiedades funcionales de solubilidad, hinchamiento, capacidad de retención de agua y de aceite y la resistencia a la digestión enzimática. Los resultados mostraron que la hidrólisis ácida fue el tratamiento más efectivo para mejorar la solubilidad y la retención de aceite de ambos almidones, debido al elevado efecto degradativo inducido por el ácido en los gránulos y la formación de estructuras helicoidales apropiadas para el atrapamiento de aceite, respectivamente. Por otra parte, el tratamiento en autoclave fue más efectivo para mejorar el hinchamiento y la retención de agua de ambos almidones, mediante el fortalecimiento de las interacciones entre los componentes moleculares del almidón. Dichas interacciones mejoraron la calidad de cristal, la cual fue responsable del incremento de la resistencia a la

digestión enzimática de ambos almidones. Además, el orden de dobles hélices afectó la resistencia a la digestión enzimática del HS modificado. En los almidones tratados por autoclave retrogradados, las moléculas de agua plastificaron las cadenas de almidón promoviendo su ordenamiento en dobles hélices mejor empacadas y regiones cristalinas. Adicionalmente, la formación de cristales de dobles hélices de amilosa homogéneos incrementó la resistencia a la digestión enzimática del AHS retrogradado, mientras que en el ANS, la recristalización de la amilopectina disminuyó dicha resistencia debido a la interferencia en la formación de cristales de amilosa homogéneos. La selección del método de modificación y condición de proceso apropiados permite impartir propiedades funcionales específicas al NS y HS. Las aportaciones científicas de este trabajo pueden contribuir al diseño de almidones modificados novedosos con funcionalidad específica.

TABLE OF CONTENTS

INDEX OF FIGURES

INDEX OF TABLES

CHAPTER 1. INTRODUCTION

Starch is a polysaccharide widely used in the industry, because of its renewability, biodegradability, low cost, and availability. Starch is industrially used as a component in food, adhesives and paper binders, textiles, chemical production, a feedstock for fermentation, and other industrial products (Ogunsona, Ojogbo, & Mekonnen, 2018). Starch is formed by the macromolecules amylose and amylopectin, which are arranged in semicrystalline granules (Warren, Gidley, & Flanagan, 2016). The ratio of both macromolecules affects the structural features of starch, which determines its functionality (Wang, Zhang, Chen, & Li, 2016).

Due to their poor functionality, native starches are not widely used for industrial applications (Trinh, 2015; Wang & Copeland, 2015), so, the structure of native starches is usually modified by chemical, physical, enzymatic and biotechnological methods or their combinations (Ogunsona et al., 2018). Acid hydrolysis and autoclaving, categorized as chemical and physical methods, respectively, have been used to modify the structure of starch to improve its functional properties (Ashwar et al., 2016; Astuti, Widaningrum, Asiah, Setyowati, & Fitriawati, 2018; Chen, Xie, Zhao, Qiao, & Liu, 2017; Hu, Xie, Jin, Xu, & Chen, 2014; Utrilla-Coello et al., 2014; Zhang, Hou, Liu, Wang, & Dong, 2019; Zhou, Ma, Yin, Hu, & Boye, 2019); however, the influence of the structure on the functionality of modified starches has not been well understood, especially because the modification methods have been applied under narrow conditions. Since the functionality of starch is a result of its structural features, a better understanding of the relationship between the structure of acid hydrolyzed and autoclaved starches and their functionality can help to design starches with desired functional properties.

Hypothetically, the starch modification under different acid hydrolysis times and autoclaving temperatures not only could improve the functionality but also could produce multifunctional starch materials potentially attractive to the industry. For this reason, in this work, two corn starches with different amylose content, normal (NS) and high amylose, Hylon VII (HS), were acid hydrolyzed and autoclaved aiming to investigate the effect on the structure. Also, the influence of the structure of modified starches on the functional properties was assessed. In chapter 2, the review of novel literature regarding starch structure and functionality is presented and in chapter 3, the materials and methods used in this work are described. The results of the research are presented in chapters 4, 5, and 6, preceded by a brief literature review related to the specific aims of this work.

The results discussed in chapter 4, describe the effect of acid hydrolysis for 3-15 days on the morphology, double-helical structure, thermal parameters, and functionality of NS and HS and to establish the relationship between structure and functionality. The aim of chapter 5 was to evaluate the influence of autoclaving at 105-135 °C on the morphology, crystallinity, double-helical structure, thermal parameters, and functionality of NS and HS. The relationship between structure and functionality, including the resistance to enzymatic digestion, was also examined. Finally, in chapter 6, the aim was to understand the structural changes and digestion resistance of starches autoclaved at 120 °C after retrogradation under controlled hydration for 7 days at 20 °C. Chapter 7, summarizes the relevant conclusions of this work.

CHAPTER 2. LITERATURE REVIEW

In this chapter, the structure and functionality of the starch will be briefly described, and the concepts of the gelatinization, pasting, and retrogradation will be reviewed, as they are related to several applications of starch. Additionally, the concept of resistant starch will be briefly reviewed, as its resistance to enzymatic digestion represents one of the most important aspects of the functionality of starch. Also, the current knowledge of the structure of high amylose starch, a type of starch with some special properties used in this study will be discussed.

2.1 STARCH STRUCTURE

Starch occurs in nature in the form of granules stored in plant tissues. It is considered as the main source of energy for humans and an important biomaterial for several industrial applications. Starch is composed mainly of amylose and amylopectin, both polymers of glucose. Most starches (normal or regular) contain 60-90% amylopectin, although there are high amylose starches with 30% amylopectin, and waxy starches virtually amylose free (Copeland, Blazek, Salman, & Tang, 2009). The proportion and organization of these macromolecules in the granule result in considerable variability, between and within species, in the shape, size, and properties of starch granules (Wang & Copeland, 2013).

2.1.1 Amylose

The amylose molecule is constituted of (1,4) linked α-D-glucopyranosyl units (Buléon, Colonna, Planchot, & Ball, 1998) and its degree of polymerization (DP) ranges from hundreds to tens of thousands. It has been established that amylose of a small molecular weight is essentially a linear molecule, whereas that of a large molecular weight is constituted by multiple extra-long chains (DP > 2730 in maize amylose), long chains (DP > 230), and immature clusters of short branch chains (DP ~ 18) as observed in Figure 1 (Ai & Jane, 2018; Takeda, Shitaozono, & Hizukuri, 1990). Amylose differs in size and structure according to the botanical source (Tester, Karkalas, & Qi, 2004).

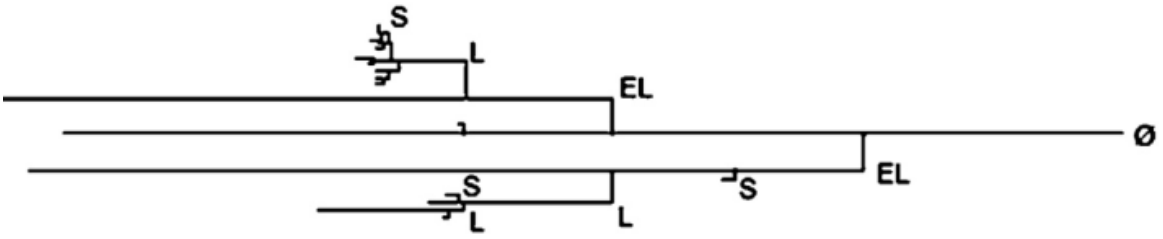

Figure 1 – Representation of the branched amylose molecule structure. (EL), extra-long; (L), long; and (S), short chains; (Ø), reducing end (Takeda et al., 1990)

2.1.2 Amylopectin

Amylopectin is a highly branched molecule formed by chains of α-D-glucopyranosyl units connected mainly by (1,4) linkages, but with 5-6% of (1,6) linkages at the branching points (Buléon et al., 1998). The DP of the branch chains of amylopectin ranges from 6 to ~ 100 (Figure 2) (Ai & Jane, 2018). The size, shape, structure, and polydispersity of the amylopectin molecule differ from the botanical source (Tester et al., 2004).

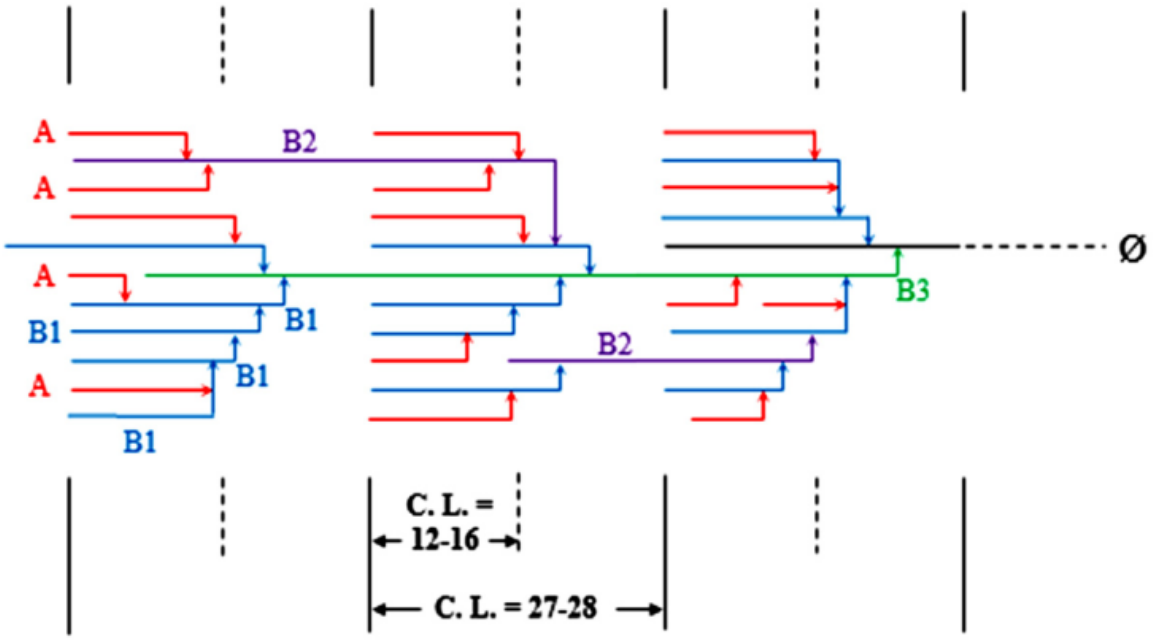

Figure 2 – Representation of an amylopectin cluster with A (–), B1 (–), B2 (–), and B3 (–) chains. The C chain is carrying the reducing end (Ø). –: α-1,4 glucan chain; →: α-1,6 linkage. C. L., chain length (Hizukuri, 1986)

2.1.3 Granular architecture

The biosynthesis of the starch granules starts at its organic center, the hilum, and the starch chains elongate radially towards the periphery by apposition (Ai & Jane, 2018). The granule's shapes are spheres, ellipsoids, polygons, platelets, and irregular tubules, with sizes of 1 μm to about 100 μm in diameter (Pérez & Bertoft, 2010; Vamadevan & Bertoft, 2015). The granules have an amorphous core surrounded by concentric semicrystalline growth rings that alternate with amorphous growth rings (Wang, Li, Copeland, Niu, & Wang, 2015). The granular core is constituted of amylose and amylopectin chains not organized into crystallites, while the periphery is predominantly composed of amylopectin interspersed with some amylose molecules (Ai & Jane, 2018; Wang, Blazek, Gilbert, & Copeland, 2012). Starch granules are organized hierarchically (Figure 3).

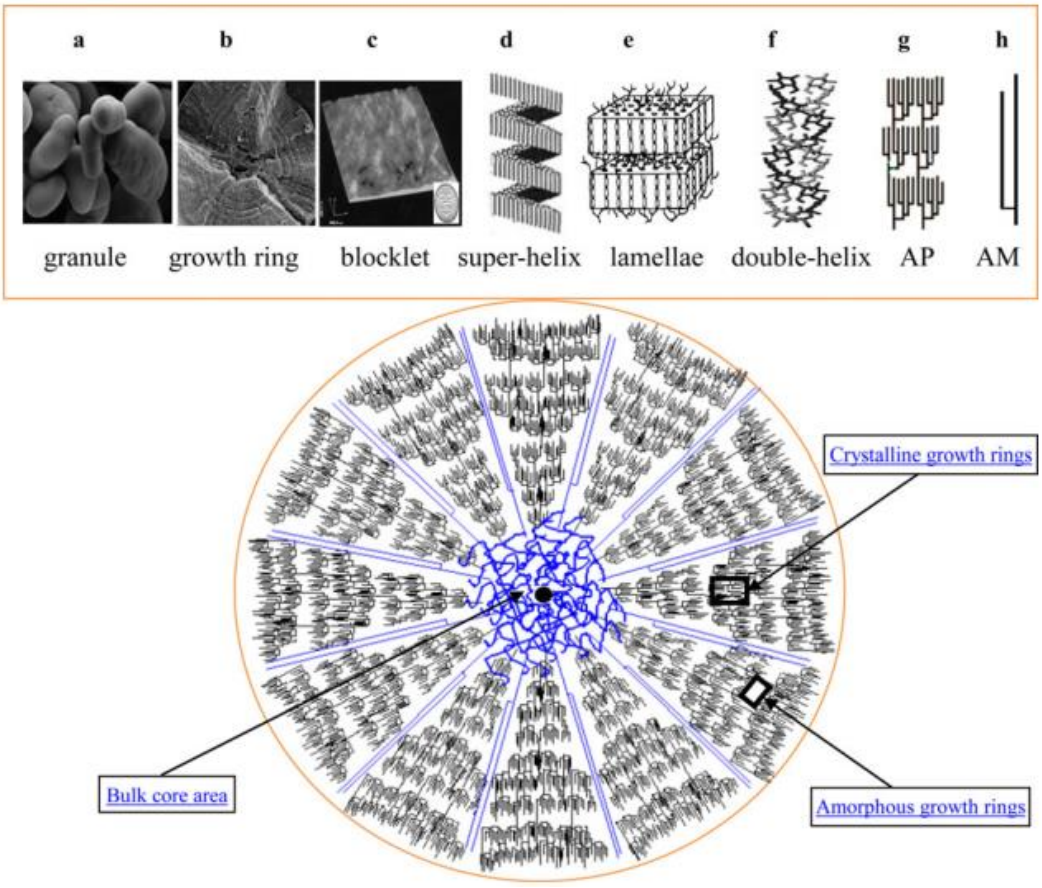

Figure 3 - The granular structure (upper) and a representative model illustrating the localization of amylose and amylopectin in the granule (lower). (a) Native pea starch granules; (b) growth rings; (c) blocklets; (d-h) superhelix, lamellar and double-helical structures, and amylopectin and amylose molecules, respectively. In the model, the blue lines represent the amylose component, while the black lines represent the amylopectin component (Wang et al., 2015)

At the highest level of structure is the granule, followed by the alternating semicrystalline and amorphous growth rings (100-500 nm). The semicrystalline growth rings are constituted of amylopectin crystallites interspersed with amylose molecules, while the amorphous growth rings are constituted of extended chains of amylopectin that interconnect the crystalline regions and interspersed amylose molecules (Wang et al., 2012). At the next levels, are the blocklets (20-500 nm) (Gallant, Bouchet, & Baldwin, 1997), the left-handed super-helices (Oostergetel & van Bruggen, 1993) and the alternating crystalline and

amorphous lamellae (9 nm) (Wang et al., 2015). The crystalline lamellae are former of clusters of amylopectin double helices, while the amorphous lamellae contain amylopectin branch points, amylopectin chains not organized into helices, and long linear amylopectin chains interconnecting the clusters (Wang & Copeland, 2013). The adjacent linear chain segments in the clusters arranged into double helices (Pfister & Zeeman, 2016), which are packed in the A-type or the B-type polymorph (Figure 4). The double-helical structure within the two polymorphs is essentially identical; however, the packing within the A-type polymorphic structure is more compact and less hydrated, while the B-type polymorphic structure is open and contains a hydrated helical channel (Tester et al., 2004). Detailed information about starch biosynthesis and structure, is available in excellent reviews of starch biosynthesis (Pfister & Zeeman, 2016) and structure (Pérez & Bertoft, 2010).

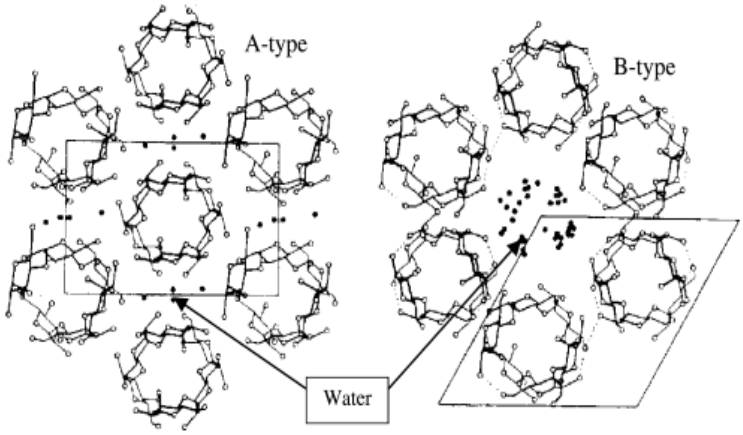

Figure 4 - A- and B-type polymorphs of amylose (Tester et al., 2004)

2.2 STARCH FUNCTIONALITY

The changes that starch granules undergo when they are thermally treated in water determine its functionality and applications in the industry (Wang & Copeland, 2015). Those changes are swelling and solubility, gelatinization, pasting, and retrogradation. Moreover, an important aspect of the functionality of starch is its susceptibility to enzymatic digestion (Wang & Copeland, 2015; Wang et al., 2015). The resistant starch, a starch fraction that passes undigested into the large intestine, brings important health benefits (Sullivan & Small, 2019).

There is a wide variety of native starches that meet the requirements for different necessities (Wang & Copeland, 2015), however, their functional limitations, such as low resistance to shear stress, poor thermal stability, a high tendency to retrogradation and its hydrophilic nature prevent its wide use in the industry (Ogunsona et al., 2018; Wang & Copeland, 2015; Zia-ud-Din, Xiong, & Fei, 2017). Therefore, the applications of starch in the industry can be expanded by using several modification methods (Zia-ud-Din et al., 2017).

2.3 PHYSICAL PROPERTIES OF STARCH IN WATER

2.3.1 Gelatinization

The granules of native starch are insoluble in water at room temperature. After heating to a specific temperature in excess of water, the starch granules undergo an irreversible transition defined as gelatinization. During this transition, the starch granules structure is disrupted (Ai & Jane, 2018; Wang & Copeland, 2013). The conceptions about gelatinization of starch granules are related to polymer science and four models; the spherulites model, the fringed micelles model, the three-phase model, and the chiral side-chain polymeric liquid crystal

model, describe their evolution over time, as reviewed by Matignon & Tecante (2017) (Figure 5). Currently, gelatinization could be defined as a non-equilibrium process dependent on high energy input, which causes the loss of the native orders in the granules. How this phenomenon occurs is influenced by the content of water, because of its plasticizer effect (Liu, Yu, Copeland, Wang, & Wang, 2019; Matignon & Tecante, 2017).

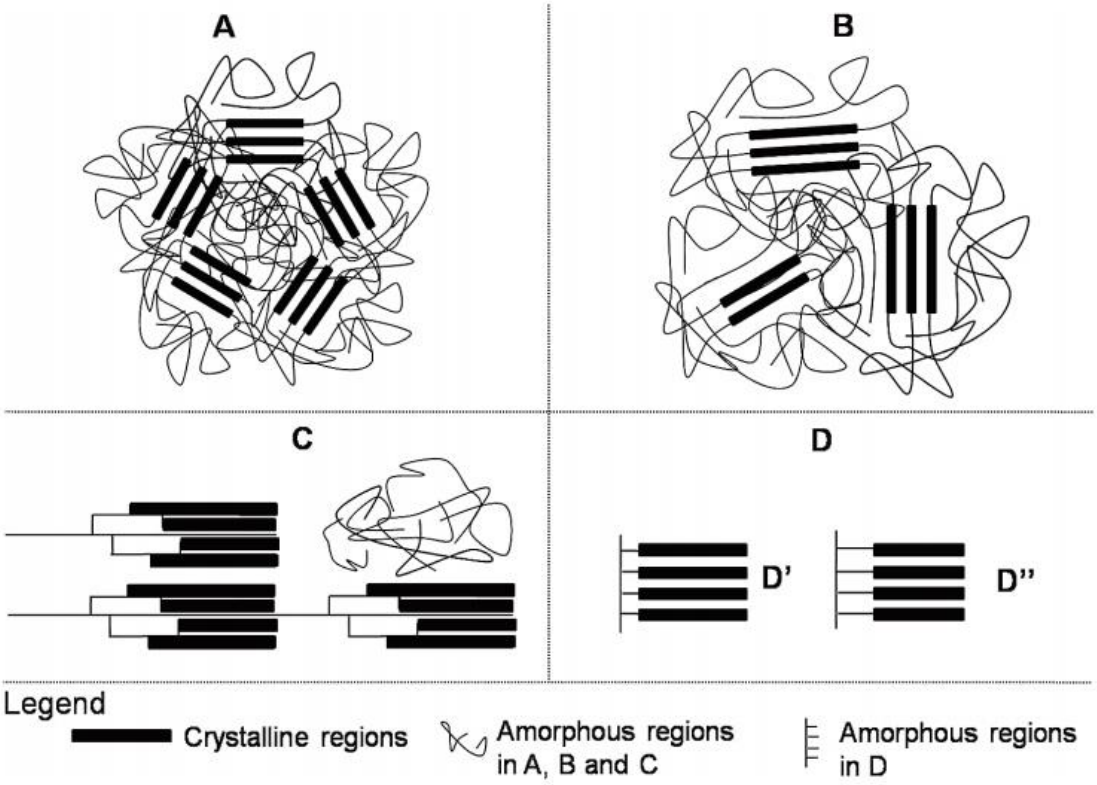

Figure 5 - Evolution of the conceptions of gelatinization of starch granules; A. The spherulites model (Meyer, Bernfeld, Boissonnas, Gürtler, & Noelting, 1949); B. The fringed micelles model (Slade & Levine, 1993); C. The three-phase model (Biliaderis, Page, Maurice, & Juliano, 1986); D. The chiral side-chain polymeric liquid crystal model, D' A-type starches and D'' B-type starches (Waigh, Gidley, Komanshek, & Donald, 2000)

Due to the polydispersity of starch granules, the gelatinization is not a sharp transition, although in general, this phenomenon occurs in a temperature range between 60 and 80 ºC for most starches (Liu et al., 2019). The gelatinization temperature generally increases when the branch chain length of amylopectin increases due to the branch chains form the double-helical crystallites of starch granules that are lost during gelatinization (Ai & Jane, 2018). Waxy starches, with short branch chains of amylopectin, gelatinized at lower temperatures, while high amylose maize starches, with longer branch chains of amylopectin, gelatinized at higher temperatures (Ai & Jane, 2018; Chen et al., 2017b). In high amylose starches, amylose forms double-helical crystallites resulting in much greater thermal stability and higher-conclusion gelatinization temperatures (Ai & Jane, 2018; Tester et al., 2004).

2.3.2 Pasting

Pasting is the combination of processes occurring after the start of gelatinization (Matignon & Tecante, 2017). During the gelatinization process, the starch granules swell, the amylose is leached from the swollen granules and the molecular components of starch are dispersed in the aqueous medium (Ai & Jane, 2018). The resulting starch dispersions, the so-called pastes can be described (Figure 6) as dispersions of swollen granules in the aqueous medium with or without leached amylose, an aqueous phase of scattered swollen granules and remnants enriched with starch macromolecular components and such components dispersed in the aqueous medium (Matignon & Tecante, 2017).

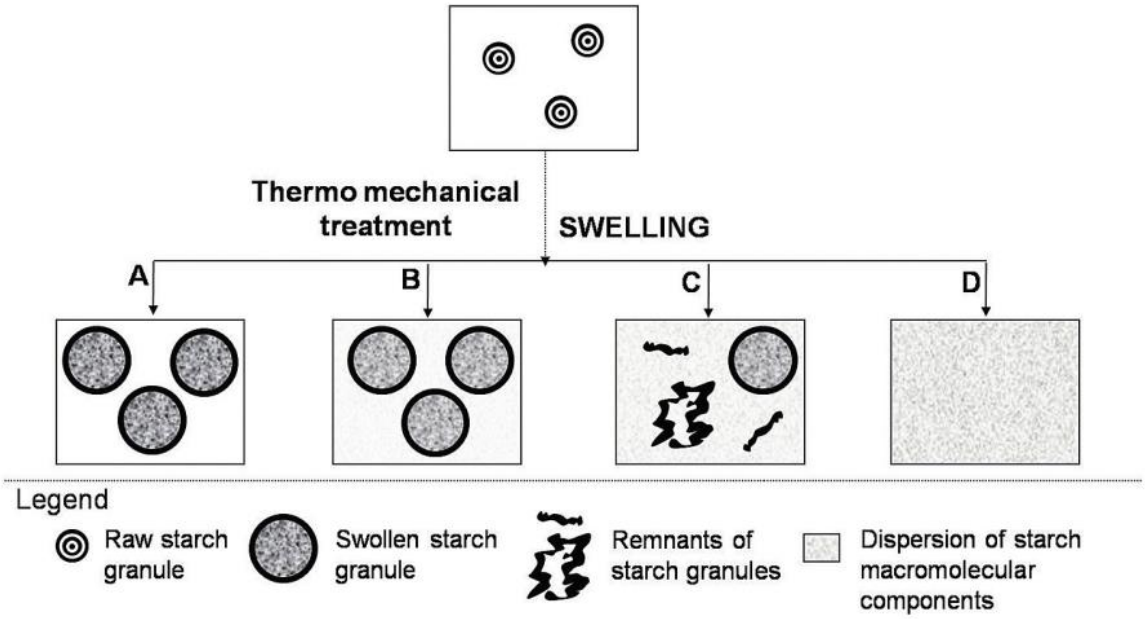

Figure 6 - Models of starch pastes; A. Swollen granules dispersed in an aqueous medium; B. Swollen granules dispersed in an aqueous medium with leached amylose; C. Swollen granules and remnants of granules dispersed in an aqueous medium with starch macromolecular components; D. Starch macromolecular components dispersed in an aqueous medium (Atkin, Abeysekera, & Robards, 1998)

2.3.3 Retrogradation

The retrogradation is defined as the reorganization of the disordered starch molecules after the gelatinization process (Matignon & Tecante, 2017). The disrupted glucan chains can gradually reassociate through hydrogen bonds into double-helical crystallites (Ai & Jane, 2018; Vamadevan & Bertoft, 2018; Wang et al., 2015). After the gelatinization, two consecutive events promote the recrystallization of starch. The first event is the nucleation, in which the starch chains form aggregates, and the second is the propagation or crystal growth, where the starch chains form double-helical crystallites (Vamadevan & Bertoft, 2018).

The amylopectin recrystallization is a long-term process, while the amylose crystallization is a short-term one (Matignon & Tecante, 2017). During retrogradation, interactions between amylopectin and amylose can occur (Lian, Cheng, Wang, Zhu, & Wang, 2018). The retrogradation of starch is enhanced by increasing the starch concentration, the amylose content, the branch chain length of amylopectin, the storage time, and storing the starch paste at 0-5 °C (Ai & Jane, 2018). An overview of the gelatinization, pasting, and retrogradation of starch, is presented schematically in Figure 7.

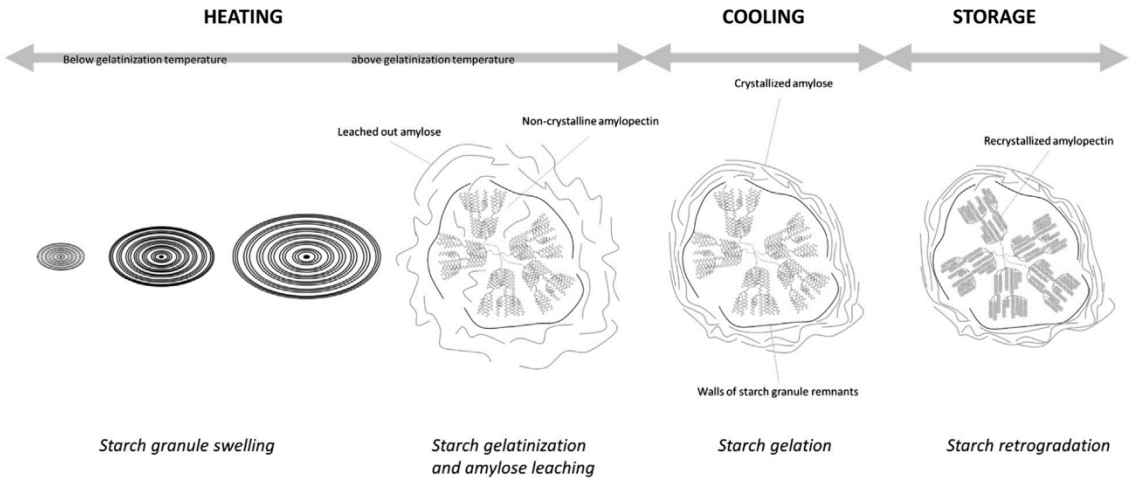

Figure 7 – Structural changes during gelatinization, pasting, and retrogradation of starch (Joye, 2018)

2.4 RESISTANT STARCH

The resistant starch term was introduced by Englyst, Wiggins, & Cummings (1982) to describe the starch part that arrives into the large intestine, where it generates a positive impact on health (Sullivan & Small, 2019). Resistant starch has been linked to physiological benefits such as prebiotic effect on microbiota, improvement of cholesterol metabolism, and prevention of ulcerative colitis and colon cancer (Tacer-Caba & Nilufer-Erdil, 2019).

According to its mechanism of resistance to enzymatic digestion, the resistant starch is classified into 5 types (RS1-RS5). RS1 is physically inaccessible starch because a physical barrier (often a cell wall) prevents the contact of enzymes with the starch granules (Sullivan & Small, 2019). In native starches, it is found the RS2, whose compact structure limits the access of digestive enzymes (Tacer-Caba & Nilufer-Erdil, 2019). RS3 is retrograded starch; it is thermally stable and it is formed in moist-heated foods (Öztürk & Mutlu, 2018; Raigond, Ezekiel, & Raigond, 2015). RS4 owes its digestion resistance to chemical modification and RS5 refers to the amylose portion of starch which has been complexed with lipids to form a helical structure that is resistant to enzymatic digestion (Amini Khoozani, Birch, & El-Din Ahmed Bekhit, 2019; Sullivan & Small, 2019; Tacer-Caba & Nilufer-Erdil, 2019). Among these RS categories, RS3 has particularly attracted attention because it preserves its nutritional functionality during cooking, which expands its applications as a food ingredient (Ma & Boye, 2018).

2.5 HIGH AMYLOSE STARCH

The high amylose starch is used in the areas of support films, foods, paper making, and medical treatments due to the strength of its granules against gelatinization and hydrolysis (Chen et al., 2017b). The high amylose starches have low crystallinity but their granules are compact without weak points or voids, which could be the reason for its resistance to gelatinization and hydrolysis; however, the reason for such a compact granule architecture is not well understood (Yang et al., 2016). The high amylose starches have small and large granules characterized by smooth surfaces. The small granules have higher contents of amylose and amylopectin long branch-chains, lower contents of amylopectin short branch-

chains, and smaller branching degrees than the large granules, which lead to a strong structure that is resistant to gelatinization (Chen et al., 2017b).

In normal or regular starches, which have been extensively studied, the supramolecular structure of the granules is attributed to the amylopectin component, while amylose is located in granules as an individual, radially oriented and randomly distributed chains, disrupting the structural order within the amylopectin crystallites (Yang et al., 2016). However, in high amylose starch, research indicated that amylose can form double-helical crystallites (Tester et al., 2004), so, it is considered that the granular periphery is constituted by double-helical crystallites of amylose and amylopectin intertwined with amylose molecules (Figure 8) (Yang et al., 2016). In contrast, the granule inner region is more crystalline but has a loosely packed structure, explaining why the gelatinization or hydrolysis starts in this region (Chen et al., 2017b; Yang et al., 2016).

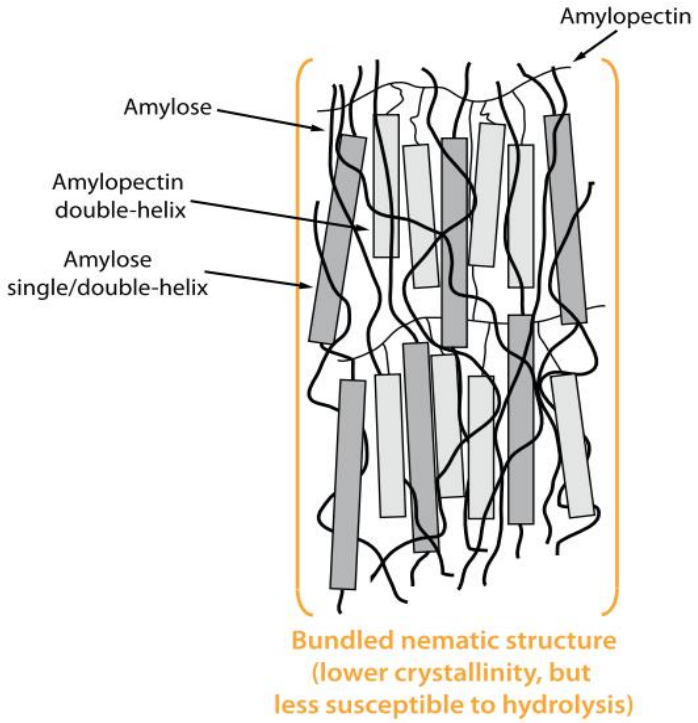

Figure 8 – Organization of the periphery in high amylose starch (proposed model) (Yang et al., 2016)

CHAPTER 3. MATERIALS AND METHODS

3.1 STARCHES

Normal (NS) and high amylose, Hylon VII (HS) corn starches were obtained from National Starch and Chemical S.A. de C.V. (Toluca, Mexico). The amylose content of the NS and HS was 27 and 70 %, respectively (O'Brien, Wang, Vervaet, & Remon, 2009). The chemicals used were of an analytical grade standard.

3.2 METHODS

3.2.1 Sample preparation

3.2.1.1 Acid hydrolysis

Acid hydrolysis was used to modify NS and HS. The starches (10 g, dry basis) were dispersed in 200 mL HCl aqueous solution (7.5% w/w). The container was stored for 15 days at 25 °C under constant stirring. Aliquots (10 mL) taken after different days (3, 6, 9, 12, and 15) were neutralized with NaOH (7.5% w/w) and centrifuged at 2000 RPM for 10 min. The supernatant was used to calculate the degree of hydrolysis (DH, Equation 1) through the determination of soluble sugars using the phenol-sulfuric acid method (Dubois, Gilles, Hamilton, Rebers, & Smith, 1956) and the precipitates were washed three times with distilled water, dried at 40 °C for 24 h and stored into sealed glass containers at 25 °C.

$$DH\ (\%) = (Soluble\ sugars/Weight\ of\ starch)\ x\ 100 \quad \text{Eq. 1}$$

3.2.1.2 Autoclaving

Suspensions of both, NS and HS (5% solids, w/v) were continuously stirred at 60 ºC for 15 min. Pregelatinized starch suspensions were autoclaved at 105, 120, and 135 ºC for 30 min, and the resultant starch pastes were dried at 40 ºC for 24 h, milled and passed through a 250-μm sieve. Autoclaved starches (water content of around 7%) were stored at room temperature in closed glass containers for further analysis.

3.2.1.3 Retrogradation of autoclaved starches

The retrogradation of autoclaved starches under controlled hydration was studied. NS and HS were autoclaved at 120 °C and labeled as ANS and AHS, respectively. ANS and AHS were conditioned at several relative humidities of equilibrium (RHeq) values at 20 °C for 7 days using acrylic containers with airtight lids containing supersaturated salt solutions of $MgCl_2$, K_2CO_3, NaBr, NaCl, KCl, $BaCl_2$, and K_2SO_4 to obtain environments of 33.1, 43.2, 59.1, 75.5, 85.1, 90.6 and 97.6 % RHeq, respectively (Fontana, 2008). The salt solutions were prepared following the standard method ASTM E104-02 (ASTM, 2012). An acrylic container with silica was used to obtain an environment of ~3% RHeq. A thin layer of starch was distributed on aluminum trays over saline solutions (Figure 9). This step is important as it allows a homogeneous interaction of water vapor molecules with the starch. The containers were placed in a chamber at 20 °C for 7 days. The water content of retrograded starches was determined gravimetrically. The samples were weighed before heated in an oven at 110 °C for 12 h to determine the dry weight. The water content (%) was measured using the weight of the hydrated sample and the dry weight (García, Pinotti, Martino, & Zaritzky, 2004).

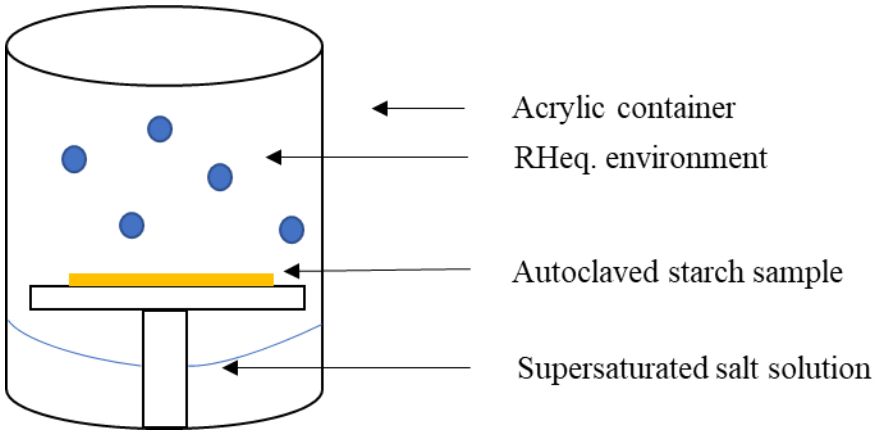

Figure 9 - Schematic representation of the conditioning of an autoclaved starch sample in an RHeq environment

3.2.2 Morphological and structural characterization

3.2.2.1 Scanning electron microscopy (SEM)

SEM is a technique used for the analysis of micro- and nanostructures with a wide range of applications (Henning & Adhikari, 2017). SEM allows studying the surface features (smooth or porous), particle size, and shape (polyhedral, oval, flattened, hexagonal) of the starch granules (Pedrosa Silva Clerici, Sampaio, & Schmiele, 2018).

Experimental procedure

The starch samples were observed using a scanning electron microscope (Phenom Pro, Phenom-World., Netherlands). The samples were attached to the aluminum sample holder using conductive double-sided carbon tape and subsequently were examined through the scanning electron microscope. The acceleration voltage was set at 5 kV and the magnification of images was 5,000x or 1,500x.

3.2.2.2 X-ray diffraction (XRD)

The XRD is used to study the structure of crystalline phases based on the ability of crystals to diffract X-rays in a characteristic manner (Epp, 2016). XRD has been used to determine the type and extent of the crystalline structure of starch (Pedrosa Silva Clerici et al., 2018). This technique detects ordered structures involving the regular and repeated arrangement of double helices of starch; however, it is not sensitive to irregularly packed structures, small chain aggregates, or isolated single helices (Ma & Boye, 2018; Wang et al., 2015).

Experimental procedure

The samples were scanned in the angular range of 2θ from 10° to 35° at room temperature in an X-ray diffractometer (D8 ADVANCE, Bruker, USA). In all tests, the operating conditions were an accelerating voltage of 20 kV, a current of 20 mA, an angular step of 0.01°, and 1 second from step to step.

The relative crystallinity (RC) of starch samples was calculated using Equation 2.

$$RC\ (\%) = \left(\frac{A_c}{(A_c + A_a)}\right) x\ 100 \qquad \text{Eq. 2}$$

where A_c represents the crystalline area and A_a the amorphous area on the X-ray diffractograms (Rabek, 1980).

3.2.2.3 Fourier transform infrared spectroscopy with attenuated total reflectance (FTIR-ATR)

The FTIR spectra have been used to monitor the changes in the double-helical order, crystallinity, starch chain conformation, and helicity during starch processing (Pratiwi, Faridah, & Lioe, 2018). The ATR accessory allows the analysis of starch samples in a range of physical forms, which makes it possible to observe spectral differences due to the level of hydration (Warren et al., 2016). The bands in the 1100-900 cm^{-1} region are sensitive to changes in starch structure, particularly the bands at 995, 1000, 1022, and 1047 cm^{-1}. The bands at 995 and 1047 cm^{-1} are related to the ordered region (Ma & Boye, 2018; Xu et al., 2019), the band at 1022 cm^{-1} to the amorphous phase (Ma & Boye, 2018; Warren et al., 2016; Xu et al., 2019) and the band at 1000 cm^{-1} to the hydrated ordered regions (Capron, Robert, Colonna, Brogly, & Planchot, 2007) of starch. This has led to the use of the ratios of 995/1022, 1047/1022 and 1000/1022 cm^{-1} to measure the degree of the double helix (DD), the degree of double-helical order (DO) and the double-helical order in hydrated samples in different studies (Capron et al., 2007; Ma, Yin, Chang, Hu, & Boye, 2018; Xu et al., 2019; Yin, Ma, Hu, Li, & Boye, 2018; Zhou et al., 2019).

Experimental procedure

The analysis of starch samples was carried out using a spectrophotometer (Spectrum GX, Perkin Elmer Inc., USA) in the range from 4000 to 650 cm^{-1} at a resolution of 4 cm^{-1}. The ratio of the intensity at 995/1022, 1047/1022, and 1000/1022 cm^{-1} were used to measure the degree of the double helix (DD), degree of order (DO), and double-helical order of starch samples in a hydrated state.

3.2.2.4 Differential scanning calorimetry (DSC)

DSC measures the energy changes in a material subjected to programmed heating or cooling (Wang et al., 2015), by measuring the temperature difference between the sample placed in a hermetically sealed container and an empty container (reference) (Pedrosa Silva Clerici et al., 2018). The transition temperatures (onset, T_o; peak, T_p; and end, T_e) and enthalpy change (ΔH) can be obtained from DSC thermograms (Pratiwi et al., 2018; Wang et al., 2015).

Experimental procedure

The thermal properties of starch samples were determined using a differential scanning calorimeter (DSC 1 STARE System, Mettler-Toledo Inc., Switzerland). For acid hydrolyzed starches, a 3 mg sample was weighed on an aluminum pan and mixed with 7 µL of distilled water. The pan was hermetically sealed and heated from 25 to 120 °C at 10 °C/min. For autoclaved starches, 5 mg of anhydrous samples (Zhou, Meng, Chen, Zhu, & Yuan, 2014) were placed in an aluminum pan which was then sealed and heated from 25 to 220 °C at 10 °C/min. Retrograded samples were analyzed in the hydrated state, using the same conditions as for autoclaved starches. The temperature of the onset (T_o), peak (T_p), end (T_e), and the enthalpy change (ΔH) were recorded using the software STARe version 9.30.

3.2.3 Functional Characterization

3.2.3.1 Water solubility index (WSI) and swelling power (SP)

The WSI and SP of starch samples were measured according to the method reported by Fonseca-Florido, Méndez-Montealvo, Velazquez, & Gómez-Aldapa (2016) with slight modifications. Mixtures of starch samples (0.5 g) and distilled water (10 mL) were stirred on a vortex for 1 min before heating at 90 ºC for 30 min. After cooling in an ice-water bath for 5 min, the samples were centrifuged at 6000 rpm for 30 min at 25 ºC. The supernatant was decanted, dried at 110 ºC for 12 h, and weighed (W_1) to calculate the WSI using Equation 3. The weight of the swollen starch sediment (W_s) was used to calculate the SP (Equation 4).

$$WSI = \frac{W_1}{0.5}\ x\ 100 \qquad \text{Eq. 3}$$

$$SP = \frac{W_s}{0.5(100-WSI)} \qquad \text{Eq. 4}$$

3.2.3.2 Water holding capacity (WHC) and oil holding capacity (OHC)

The WHC and OHC of starch samples were determined following the method described by Ashwar et al. (2016) with slight modifications. Mixtures of starch samples (0.5 g) and distilled water or corn oil (10 mL) were stirred on a vortex for 1 min and then centrifuged at 4400 rpm for 10 min at 25 °C. The supernatant was removed and the sediment (W_s) was weighed to calculate the WHC or OHC using Equation 5.

$$WHC/OHC = \frac{W_s-0.5}{0.5}\ x\ 100 \qquad \text{Eq. 5}$$

3.2.3.3 Resistant starch (RS)

The RS content of starch samples was measured following the method 32-40 (AACC, 2000). The kit from Megazyme, K-RSTAR 08/18, was used to carry out the analysis.

3.3 STATISTICAL ANALYSIS

The mean and the standard deviation of the triplicate experiments were calculated and analysis of variance (ANOVA) with a level of significance of 5% was performed. The Tukey test was applied to determine differences between means. Also, a correlation analysis (Pearson correlation coefficients) was conducted to establish the relationship between the functional properties and the structural features of modified starches using the Statistica v7 software.

CHAPTER 4. DOUBLE HELICAL ORDER AND FUNCTIONAL PROPERTIES OF ACID-HYDROLYZED CORN STARCHES WITH DIFFERENT AMYLOSE CONTENT

4.1 INTRODUCTION

The acid hydrolysis of starch is carried out by the treatment of starch granules with dilute aqueous or alcoholic solutions of mineral acid (hydrochloric or sulphuric acid) below the gelatinization temperature for different periods. Once the desired degree of hydrolysis is achieved, the resultant acid-hydrolyzed starch is recovered by neutralizing the acid solution with an alkali followed by washing or only by washing until neutrality, and subsequent drying (Wang & Copeland, 2015).

In the beginning, the acid acts on the granular surface and then attacks the loosely-packed amorphous regions within starch granules and degrades the molecular components of starch. The preferential hydrolysis of the amorphous regions increases the proportion of crystalline regions (Chen et al., 2017a).

Wang & Copeland (2015) mentioned that the hydrolysis kinetics of starch granules can be monitored in two ways: the soluble sugar content in the solution and the recovery yield of insoluble residues. Additionally, they also mentioned that most starches hydrolyze in two stages: initially, they present a relatively fast rate that could be attributed to the hydrolysis of the amorphous regions within starch granules followed by a slower rate in which it is assumed that the amorphous and crystalline regions are concomitantly hydrolyzed. The oxygen in the glycosidic bond is attacked by the hydroxonium ion, hydrolyzing the linkage (Pratiwi et al., 2018).

The acid hydrolysis modifies the structural features of starch and therefore, its functionality. There is available literature about the effect of this process on the structure and functionality of starch (Chen et al., 2017a; Utrilla-Coello et al., 2014; Wang et al., 2012; Zhang et al., 2019); however, scarce information has been published describing the relationship between structural changes of acid hydrolyzed starches and their functionality. In this work, NS and HS were submitted to hydrolysis with HCl for 15 days aiming to evaluate the changes on WSI, SP, WHC, and OHC as a function of hydrolysis time and to describe the structural changes using FTIR-ATR and DSC.

4.2 HYDROLYSIS KINETIC

The degree of hydrolysis (DH) of NS and HS is shown in Figure 10.

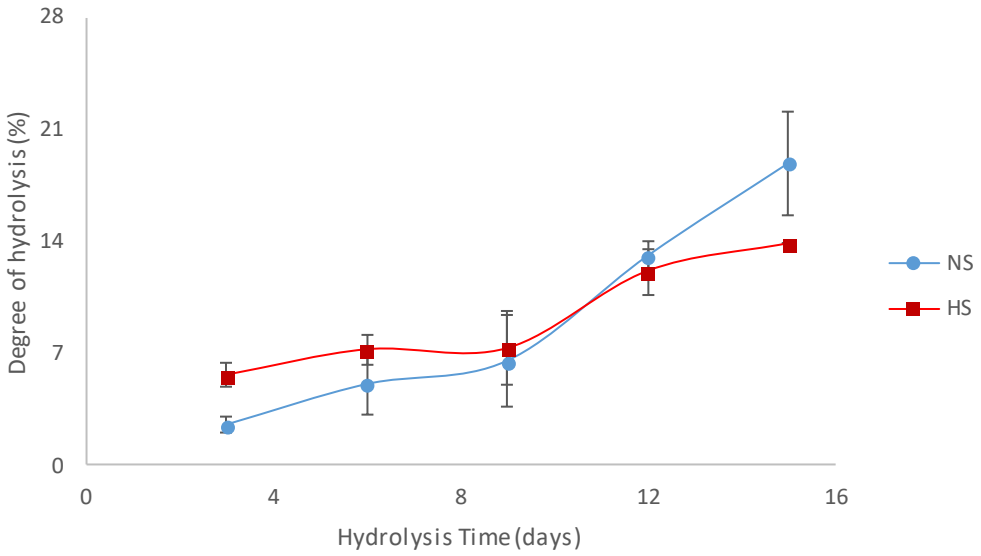

Figure 10 – Hydrolysis kinetics of corn starches during 15 days

The highest DH reached was around 20% (NS) after 15 days of acid hydrolysis. The relatively fast initial rate of hydrolysis of both starches is most probably related to the degradation of the amorphous regions in the starch granules (Wang et al., 2012). Amorphous regions are more accessible to acid attack due to the loose packing of starch chains compared to that of the crystalline regions (Robin, Mercier, Charbonn, & Guilbot, 1974; Kainuma & French, 1971). Also, the degradation of the amorphous regions is affected by the granule size, superficial pores, amylose content, and the amount of amylose-lipid complexes. On the other hand, the second stage of hydrolysis is affected by the amylopectin content, the distribution of α-(1,6) branches between the amorphous and crystalline lamellae and the degree of compaction of the double helices within the crystallites (Le Corre, Bras, & Dufresne, 2010; Wang & Copeland, 2015).

HS had a high DH at 9 days of acid hydrolysis; however, it was more difficult to hydrolyze in the final step that NS, which could be attributed to the high extent of starch inter-chain associations resulting in a more compactly organized amorphous region (Wang & Copeland, 2015).

4.3 GRANULAR MORPHOLOGY

The morphology of native and acid hydrolyzed starches at different days is shown in Figure 11.

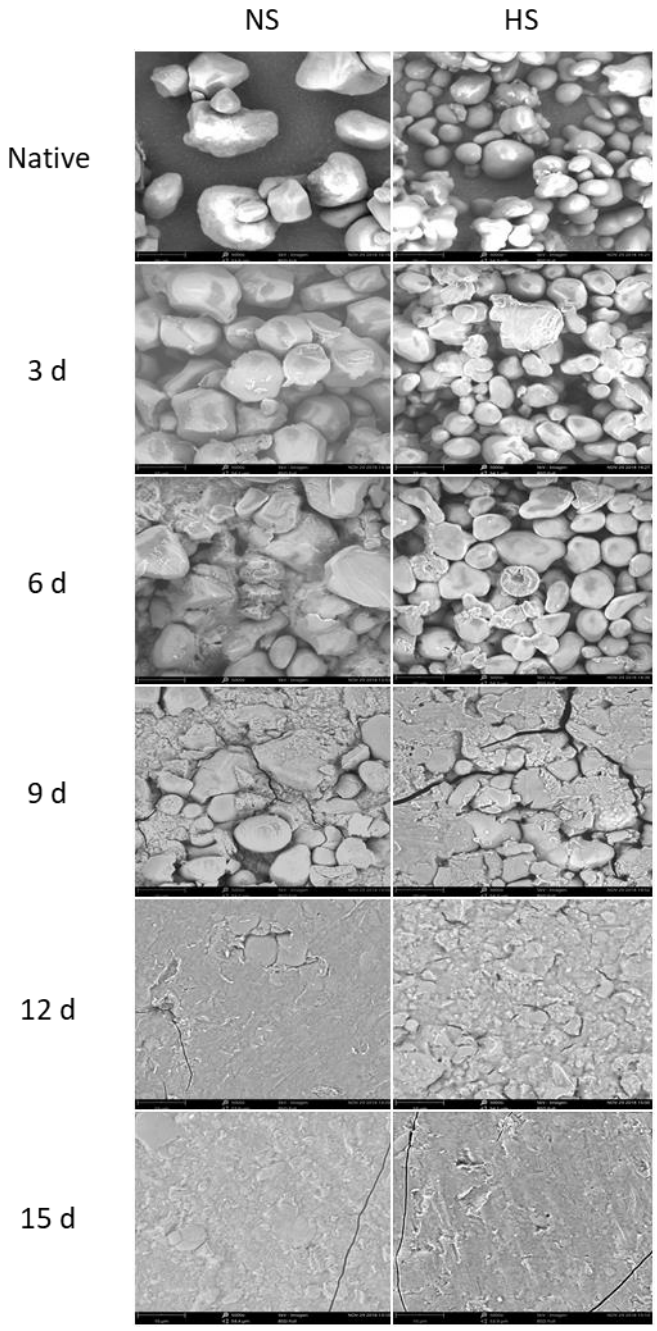

Figure 11 – SEM images of native and acid hydrolyzed starches at different times

NS displayed large and polygonal granules, while HS showed spherical, irregular, and elongated granules with heterogeneous sizes. Similar granular morphologies were reported by Chen et al. (2017b), Lin et al. (2016), and Yang et al. (2016). After 3 days of exposure to acid, the granule surface of NS and HS was considerably damaged. 6 days of acid hydrolysis caused severe corrosion resulting in cracks on the granule surface and breaking of the starch granules. In the micrographs, granule fragments were observed, showing a well-defined concentric growth-ring structure as those described by Wang et al. (2012). After 9 days of hydrolysis, few granules remained intact. The acid treatment for 12 days led to the disruption of the granular structure in both starches and the remnant structures adhered together to form a continuous network structure. NS presented a smooth surface compared to HS. The continuous network was attributed to the reorganization of the starch molecules into a helical complex matrix which could modify the functional properties of NS and HS.

4.4 DEGREE OF DOUBLE HELIX AND ORDER

The FTIR spectra of native and acid hydrolyzed starches are shown in Figure 12.

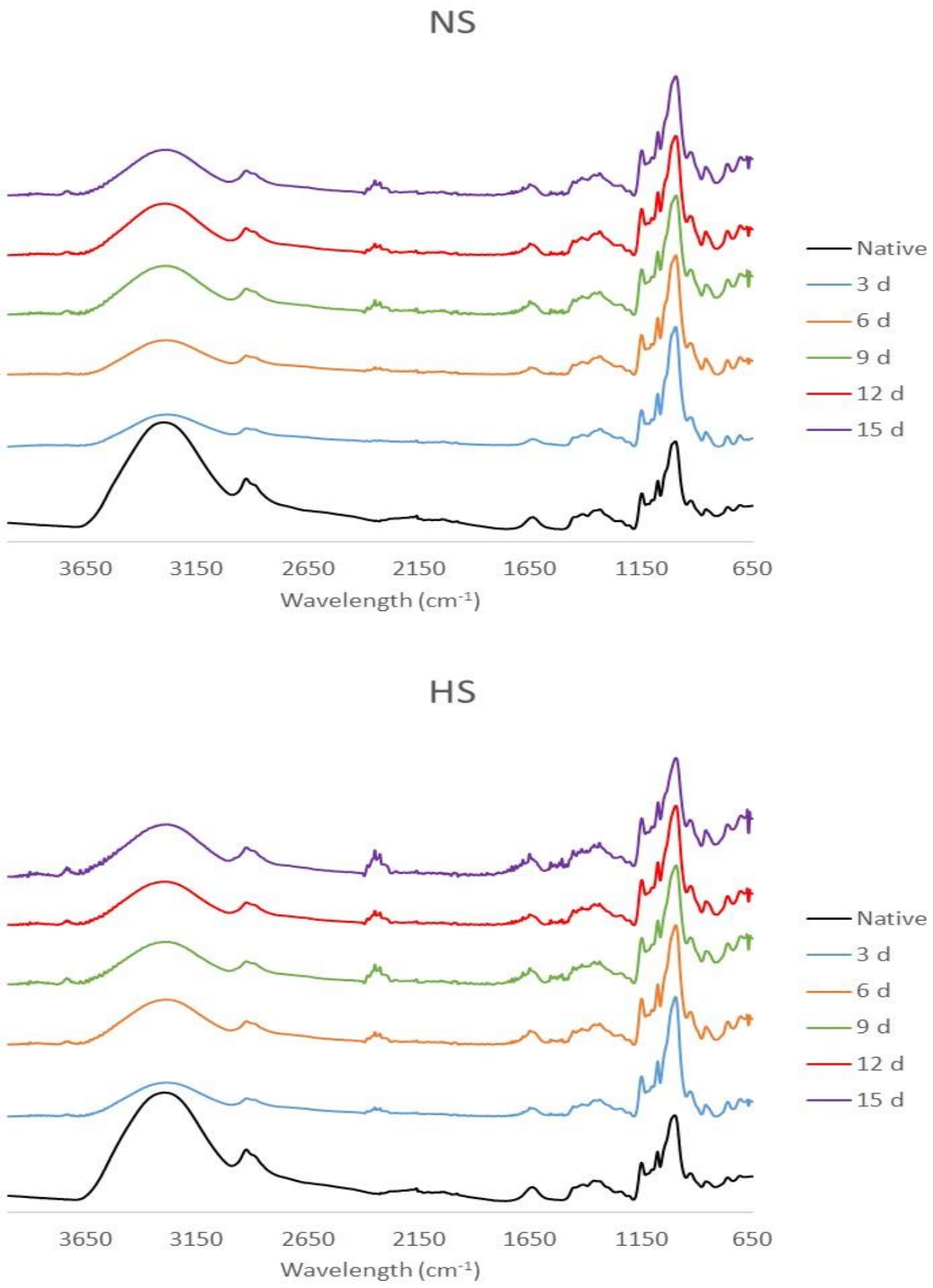

Figure 12 – FTIR spectra of native and acid hydrolyzed starches at different times

The intensities of the peaks in the 1100-900 cm^{-1} spectra region changed after hydrolysis treatment, suggesting variations in the degree of the double helix (DD) and degree of order (DO). The ratios of 995/1022 and 1047/1022 cm^{-1} were used to quantify the DD and DO, respectively (Table 1).

Table 1 – DD and DO of native and acid hydrolyzed starches

Sample	DD (995/1022 cm^{-1})	DO (1047/1022 cm^{-1})
	NS	
Native	1.1027	0.7441
3 d	1.1972	0.6386
6 d	1.1896	0.6646
9 d	1.1728	0.6963
12 d	1.2039	0.7100
15 d	1.1873	0.7123
	HS	
Native	1.0864	0.7349
3 d	1.2115	0.6350
6 d	1.2045	0.6691
9 d	1.1708	0.6994
12 d	1.1941	0.6925
15 d	1.1814	0.7941

NS and HS showed slight differences regarding the DD behavior as a function of the acid hydrolysis time. Initially, the acid process increased the double-helical structure, which could be due to the preferential hydrolysis of amorphous regions and the retrogradation of free amylose that is released (Morrison, Tester, Gidley, & Karkalas, 1993; Wang & Copeland, 2015). The cleavage of some of the amylose chains running through the amorphous regions may promote a reorganization of the newly released chain ends into double helices, extending the double-helical structure of both starches.

On the other hand, the acid hydrolysis decreased the DO value of both starches, except for acid hydrolyzed HS at 15 days. This trend reflects that acid hydrolysis decreased the compaction density between double helices, which suggests that the acid could have a degrading effect on the double-helical order of the native starches. However, through the evolution of the acid hydrolysis, the DO value increased in both starches, maybe due to the formation of short linear chains (Chen et al., 2017a) that compacted better together or to the rearrangement of decoupled double helices. These phenomena could have resulted in the high compaction density of double helices observed in acid hydrolyzed HS at 15 days.

4.5 THERMAL PROPERTIES

The thermal parameters of native and acid hydrolyzed starches are shown in Table 2.

Table 2 - Thermal parameters of native and acid hydrolyzed starches

Sample	T_o (°C)	T_p (°C)	T_e (°C)	ΔT (°C)	ΔH (J/g)
			NS*		
Native	$62.2^{b} \pm 0.5$	$70.1^{b} \pm 0.0$	$80.4^{a} \pm 0.8$	$18.2^{c} \pm 1.0$	$14.1^{a} \pm 0.0$
3 d	$63.6^{a} \pm 0.2$	$73.2^{a} \pm 0.1$	$82.2^{a} \pm 0.3$	$18.6^{c} \pm 0.5$	$8.6^{b} \pm 0.2$
6 d	$53.2^{c} \pm 0.1$	$69.4^{b} \pm 1.5$	$81.7^{a} \pm 1.0$	$28.4^{a} \pm 1.1$	$6.0^{c} \pm 0.6$
9 d	$48.0^{f} \pm 0.0$	$56.5^{e} \pm 0.2$	$75.9^{b} \pm 0.5$	$27.8^{a} \pm 0.5$	$2.6^{d} \pm 0.0$
12 d	$49.1^{e} \pm 0.0$	$60.6^{c} \pm 0.0$	$71.7^{c} \pm 0.0$	$22.6^{b} \pm 0.0$	$1.8^{e} \pm 0.0$
15 d	$50.9^{d} \pm 0.4$	$59.2^{d} \pm 1.0$	$67.5^{d} \pm 4.0$	$16.6^{c} \pm 3.5$	$0.5^{f} \pm 0.0$
			HS		
Native	$67.6^{a} \pm 0.4$	$84.0^{a} \pm 0.8$	$104.5^{b} \pm 0.6$	$36.9^{a} \pm 1.1$	$9.1^{b} \pm 0.3$
3 d	$68.8^{a} \pm 3.3$	$88.3^{b} \pm 0.1$	$102.8^{a} \pm 0.4$	$33.9^{a} \pm 2.9$	$4.8^{a} \pm 1.2$
6 d	ND	ND	ND	ND	ND
9 d	ND	ND	ND	ND	ND
12 d	ND	ND	ND	ND	ND
15 d	ND	ND	ND	ND	ND

For each starch, means with different letters in the same column are significantly different ($P < 0.05$). ND: Not detected. * Reported by Valenzuela-Díaz (2019).

An endothermic transition at 70.1 °C and 84.0 °C (T_p values) was detected for NS and HS, respectively. The main endothermic transition peak of acid hydrolyzed starch detected by DSC is generally shifted to higher temperatures compared to native starch, which reflects an increase in gelatinization temperature (T_p) as a result of the improved molecular order or crystallinity in acid-hydrolyzed starch (Wang & Copeland, 2015). In the present study, this behavior was observed for NS at 3 days of treatment; after that, a decrease was detected,

which could be explained by the disruption of starch granules, forming a continuous network as observed in the SEM images (Figure 11) taking less energy to disorganize the system. In HS, no transitions were detected after 3 days of hydrolysis.

Acid hydrolyzed starches showed a broadening of the transition temperature range (ΔT), probably due to the heterogeneity of the crystallites formed from different entities after hydrolysis, including the crystalline amylopectin side chains and retrograded amylose (Wang & Copeland, 2015). The increase of ΔT in NS took place from day 3 to day 12; meanwhile, on day 15, the ΔT decreased, indicating that all disrupted material was more homogeneous but not more ordered, as shown by the low value of ΔH.

The effect of acid hydrolysis on the ΔH of gelatinization is inconsistent. In the literature, the ΔH decreased when the acid hydrolysis time increased, which has been explained considering that ΔH is mainly due to amorphous regions that are preferentially hydrolyzed. Also, it has been mentioned that the enthalpy could change due to the dissolution of short chains which is not measured by DSC. However, some researchers reported an increase in ΔH after acid hydrolysis, attributed to an increase in the content of double helices or crystallinity (Wang & Copeland, 2015). In this study, ΔH decreased with the evolution of the acid hydrolysis, suggesting the reduction of the amorphous regions in NS.

4.6 WATER SOLUBILITY INDEX (WSI) AND SWELLING POWER (SP)

The WSI of native and acid hydrolyzed starches is shown in Figure 13.

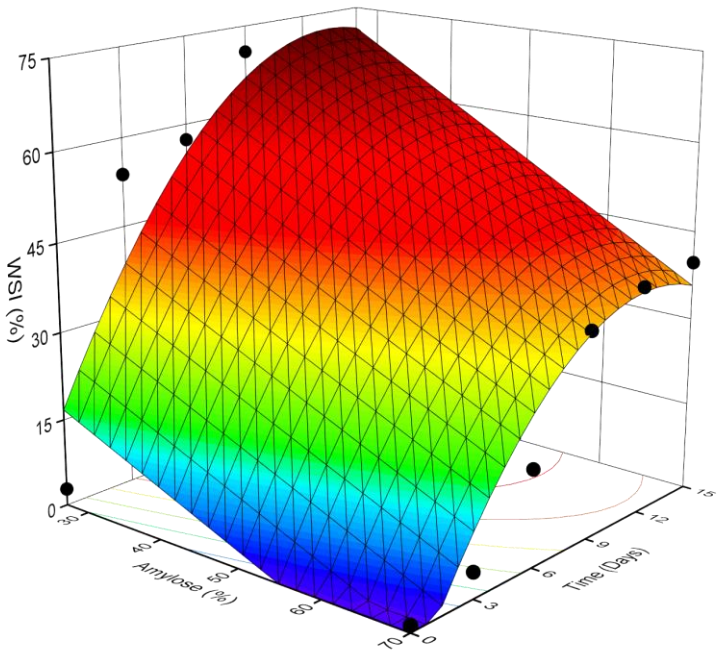

Figure 13 – WSI of native and acid hydrolyzed starches

The starch solubility is a result of the leaching of starch molecules from the granules during swelling (Ashwar et al., 2016; Biliaderis, 2009). The leached material is mainly amylose, although amylopectin can also solubilize depending on the type of the starch and the intensity of the thermal conditions employed (Biliaderis, 2009). The WSI of NS and HS was 2.8 and 1.2%, respectively. The acid hydrolysis increased the WSI in both starches, from 2.8% to 70.5% (9 days) in NS (Valenzuela-Díaz, 2019) and from 1.2% to 39.7% (15 days) in HS. NS reached higher values after acid treatment.

The SP of native and acid hydrolyzed starches is shown in Figure 14.

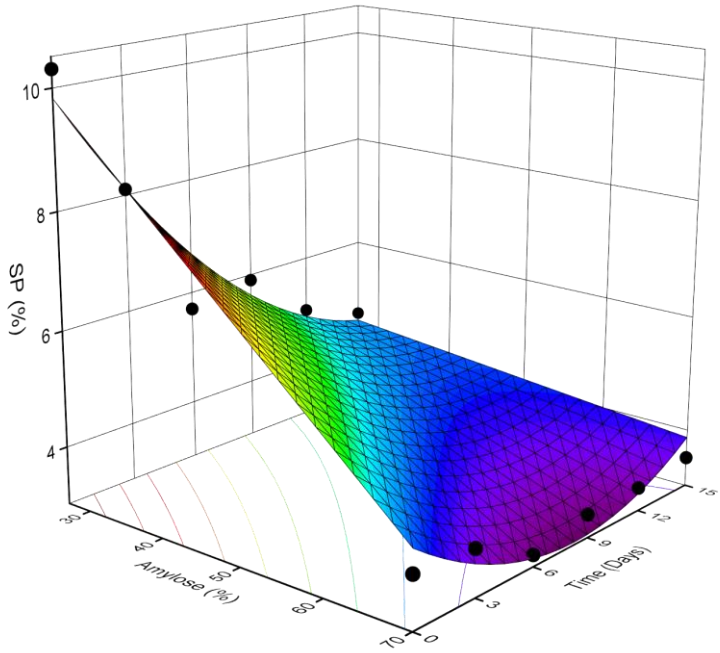

Figure 14 - SP of native and acid hydrolyzed starches

The granules of NS swelled more (10.3%) than the granules of HS (3.9%), which can be explained by the difference in the amylopectin content. The intact amylopectin forms a structural network that is related to the capability of the starch granule to entrap water and swell (Wang & Copeland, 2015). The acid hydrolysis had a bigger effect on the SP of NS, decreasing it from 10.3% to 4.6% (15 days) (Valenzuela-Díaz, 2019), whereas in HS, the SP slightly decreased from 3.9% to 3.2% (6 days).

4.7 WATER HOLDING CAPACITY (WHC) AND OIL HOLDING CAPACITY (OHC)

The WHC of native and acid hydrolyzed starches is shown in Figure 15.

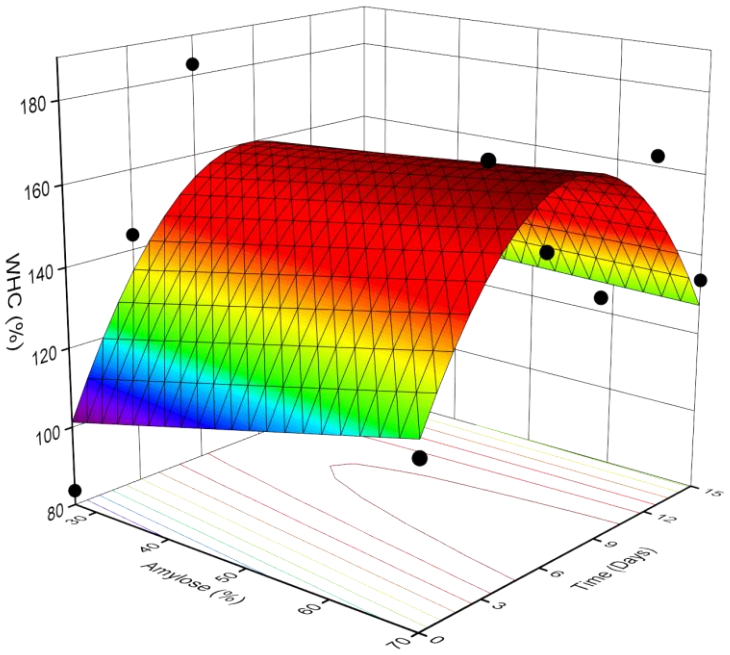

Figure 15 - WHC of native and acid hydrolyzed starches

The WHC of NS and HS was 83.6 and 119.2%, respectively. After the acid hydrolysis, the WHC increased from 83.6% to 182.8% (6 days) in NS (Valenzuela-Díaz, 2019) and from 119.2% to 178.0% (3 days) in HS. An initial increase of WHC was noticed for both starches but further increase in the acid hydrolysis time reduced the functional property.

The OHC of native and acid hydrolyzed starches is shown in Figure 16.

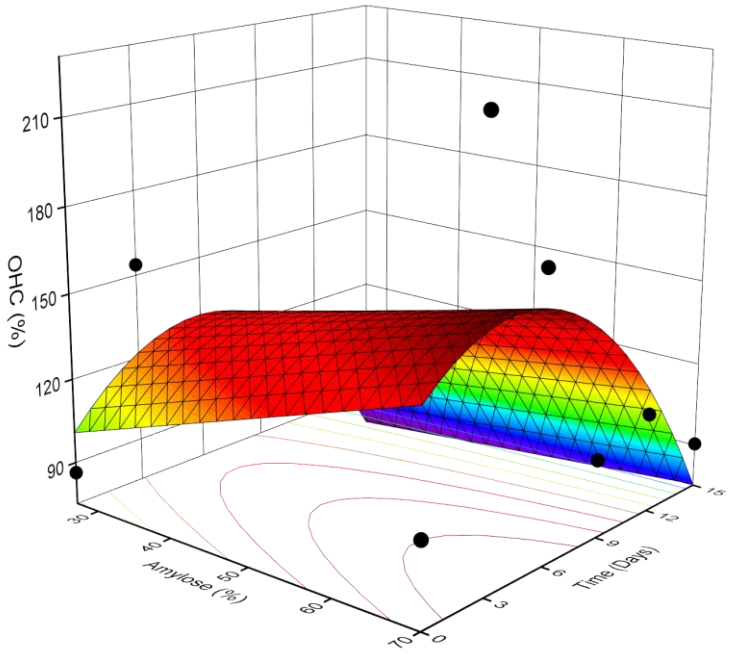

Figure 16 - OHC of native and acid hydrolyzed starches

NS exhibited a lower OHC (86.3%) than HS (104.4%). It has been hypothesized that the capability of starch to hold the oil could be attributed to the oil entrapment in a porous starch structural matrix through capillary forces or inside helical structures of amylose and amylopectin due to the formation of glucan-lipid complexes (Ashwar et al., 2016). The higher OHC of HS found in this work could be related to its high amylose content. Amylose has a unique capability to form complexes with a variety of complexing agents, including lipids (Pérez & Bertoft, 2010). The OHC increased from 86.3% to 153.7% in NS (Valenzuela-Díaz, 2019) and from 104.4% to 227.7% in HS after 3 days of acid hydrolysis. After this acid

hydrolysis time, a reduction in the OHC was observed, exhibiting lower values than native starches at extended acid hydrolysis times.

4.8 FUNCTIONAL PROPERTIES RELATED TO STRUCTURE OF ACID HYDROLYZED STARCHES

To identify the relationship between the functional properties and the structural features of native and acid hydrolyzed starches, a correlation analysis was carried out. The analysis was segmented by starches, Tables 3 and 4 correspond to NS, and Tables 5 and 6 to HS. The first Table for each starch shows the results of the correlation analysis that was performed including the native and modified starches. In the second Table, the results of the analysis performed only with the modified starches are shown. Due to the impossibility of obtaining information about the gelatinization of the modified HS, its functional properties were tried to correlate with the DD and DO values. In the next sections, the relationships will be discussed.

Table 3 - Correlation matrix between the data on functional properties and the structural parameters of native and modified NS

	WSI	SP	WHC	OHC
DD	0.89	-0.78	0.75	0.29
DO	-0.45	0.16	-0.73	-0.90
T_o	-0.72	0.86	-0.44	0.46
T_p	-0.60	0.69	-0.11	0.58
T_e	-0.51	0.68	0.10	0.73
ΔT	0.36	-0.34	0.70	0.24
ΔH	-0.93	0.97	-0.55	0.25

Table 4 - Correlation matrix between the data on functional properties and the structural parameters of modified NS

	WSI	SP	WHC	OHC
DD	-0.54	0.11	-0.30	-0.06
DO	0.90	-0.90	-0.46	-0.97
T_o	-0.84	0.87	0.04	0.81
T_p	-0.98	0.73	0.40	0.79
T_e	-0.82	0.79	0.68	0.92
ΔT	0.00	-0.07	0.76	0.14
ΔH	-0.93	0.90	0.44	0.95

Table 5 - Correlation matrix between the data on functional properties and the double-helical structure of native and modified HS

	WSI	SP	WHC	OHC
DD	0.35	-0.57	0.82	0.53
DO	0.44	0.05	-0.76	-0.82

Table 6 - Correlation matrix between the data on functional properties and the double-helical structure of modified HS

	WSI	SP	WHC	OHC
DD	-0.82	0.28	0.83	0.88
DO	0.78	-0.19	-0.80	-0.81

4.8.1 Water solubility index (WSI) and swelling power (SP)

From Table 3, after the modification of NS, the WSI was positively correlated to DD with an r value of 0.89. In acid hydrolyzed starches, the WSI was positively correlated to DO with an r value of 0.90 (Table 4). On the other hand, in HS, the WSI was not correlated to DD or DO (Table 5) after acid hydrolysis. In modified starches, the WSI was positively correlated to DO with an r value of 0.78 (Table 6).

The increased WSI observed (Figure 13) after acid hydrolysis could be attributed to the granular degradation, which resulted in the extension of the double-helical structure compared to native starches and a higher double-helical order when the acid hydrolysis time increased (Table 1). The water solubility of starch has been used as a degradation indicator of molecular components (Jagannadham, Parimalavalli, & Surendra Babu, 2017).

The SP was positively correlated to T_o, T_p, T_e, and ΔH in NS after acid hydrolysis, with r values of 0.86, 0.69, 0.68, and 0.97, respectively (Table 3). In modified starches, the SP was positively correlated to T_o, T_p, T_e, and ΔH, with r values of 0.87, 0.73, 0.79, and 0.90, respectively (Table 4). In HS, the SP was not correlated to DD or DO after the acid hydrolysis or in the modified starches (Tables 5 and 6).

The results suggest that after acid hydrolysis, the amylopectin structure was disrupted, an intact network cannot be formed and the damaged chains tend to dissolve instead to swell during heating in water (Wang & Copeland, 2015), as reflected by the decreasing of the SP values found in this study (Figure 14). This behavior can be explained considering that the water penetrates more readily into the disrupted starch granules (Figure 11).

4.8.2 Water holding capacity (WHC) and oil holding capacity (OHC)

According to Table 3, in NS the WHC was positively correlated to DD and ΔT with r values of 0.75 and 0.70, respectively after acid hydrolysis, whereas, in the modified starches, the WHC was positively correlated to T_e and ΔT with r values of 0.68 and 0.76, respectively (Table 4). In HS, the WHC was positively correlated to DD after the modification and in the acid hydrolyzed starches, with r values of 0.82 and 0.83, respectively. Interestingly, the WHC was negatively correlated to DO after the modification and in the acid hydrolyzed starches with r values of -0.76 and -0.80, respectively (Tables 5 and 6).

The increased WHC observed after the acid hydrolysis (Figure 15) in both starches could be due to a change in the molecular structure or any other mechanisms resulting in easier mobility of the starch (Jagannadham et al., 2017). Moreover, in HS, the increased double-helical order through the evolution of the acid hydrolysis (Table 1) could have worked as a barrier, restricting the accessibility and the hold of the water.

The OHC in NS was positively correlated to T_e with an r value of 0.73 after acid hydrolysis (Table 3). In the modified starches, the OHC was positively correlated to T_o, T_p, T_e, and ΔH with r values of 0.81, 0.79, 0.92, and 0.95, respectively (Table 4). In HS, the OHC was negatively correlated to DO with an r value of -0.82 after the modification (Table 5), whereas in the acid hydrolyzed starches, the OHC was positively correlated to DD with an r value of 0.88 but negatively correlated to DO with an r value of -0.81(Table 6).

The behavior of OHC after the acid hydrolysis (Figure 16) could be related to the availability of suitable helical structures for the entrapment of oil (Ashwar et al., 2016). However, with the increased acid hydrolysis time, the OHC values decreased as the double helices were able to have a more-compacted structure as demonstrated by the FTIR results (Table 1), favoring the reorganization of the structural matrix but limiting the penetration of oil.

4.9 CONCLUSIONS

NS and HS reached around 20% and 14%, respectively of DH after 15 days of acid hydrolysis. A complete granular structure disruption was reached in both starches and NS presented a smoother surface. Acid hydrolysis extended the double-helical structure of both starches and increased the double-helical order of hydrolyzed HS at 15 days, through the formation of shorter linear chains that compacted better or the rearrangement of decoupled double helices, as demonstrated by the FTIR results. There was a decrease in ΔH of gelatinization reflecting the degrading effect of the hydrolysis process on the amorphous region of NS as the treatment time increased. The acid hydrolysis can be used to change the functionality of NS and HS, through selecting a suitable time for a specific requirement. The results obtained in this study can help to understand more in-depth the effects of acid hydrolysis on the structure and functionality of corn starches with different amylose content, which can be useful when the modified starch is used as an ingredient.

CHAPTER 5. STRUCTURE AND FUNCTIONALITY OF AUTOCLAVED CORN STARCHES WITH DIFFERENT AMYLOSE CONTENT

5.1 INTRODUCTION

Among the physical methods used for starch modification, autoclaving is a widely-used process that consists in a thermal treatment at a temperature higher than 100 °C in excess of water to reach the gelatinization and disruption of the granular structure in starch (Chen et al., 2017b; Pratiwi et al., 2018). The resulting starch paste is cooled, leading to the formation of double-helical aggregates (Amini Khoozani et al., 2019). Those changes affect the morphology, the crystallinity, and the double-helical order of starch (Astuti et al., 2018; Pratiwi et al., 2018; Zhou et al., 2019).

The autoclaving treatment leads to the loss of the granular morphology of native starch, as a result of the gelatinization that occurs during the process (Pratiwi et al., 2018). After cooling and storage, gelatinized starch forms a B-type crystalline structure, involving the recrystallization of amylose and amylopectin (Ding, Zhang, Tan, Fu, & Huang, 2019; Pratiwi et al., 2018). When starch granules are autoclaved, the RC decreases, as observed in waxy wheat starch (Hu et al., 2014) and pea starch (Ma et al., 2018; Zhou et al., 2019), reflecting the melting of the crystalline structure of starch granules.

The double-helical structure of starch seems to increase after autoclaving treatment. This trend was observed in cowpea (Ratnaningsih, Suparmo, Harmayani, & Marsono, 2020), pea (Ma et al., 2018) and field pea (Zhou et al., 2019) starches modified by autoclaving and in the starch isolated from chickpea, navy bean, yellow field pea (Xu et al., 2019) and lentil (Yin et al., 2018) autoclaved seeds.

On the other hand, in the studies conducted by Xu et al. (2019), Yin et al. (2018), and Zhou et al. (2019), the double-helical order exhibited an opposite trend, decreasing after the autoclaving treatment. However, Ma et al. (2018) reported that the packing density of double helices of pea starch became more compact after the modification.

Because autoclaving causes structural changes in starch, its functional properties can be modified. Some papers deal with the effect of autoclaving on the starch structure and functionality (Astuti et al., 2018; Pratiwi et al., 2018; Zhou et al., 2019); however, to the best of our knowledge, the changes on starch functional properties and their relationship with the starch structure modified by the autoclaving process have not yet been well revealed. In this work, NS and HS were autoclaved at 105, 120, and 135 °C aiming to evaluate the effect on the functional properties WSI, SP, WHC, OHC and RS, and to establish the relationship with the structural changes assessed by XRD, FTIR-ATR, and DSC.

5.2 GRANULAR MORPHOLOGY

The micrographs of native and autoclaved starches are shown in Figure 17.

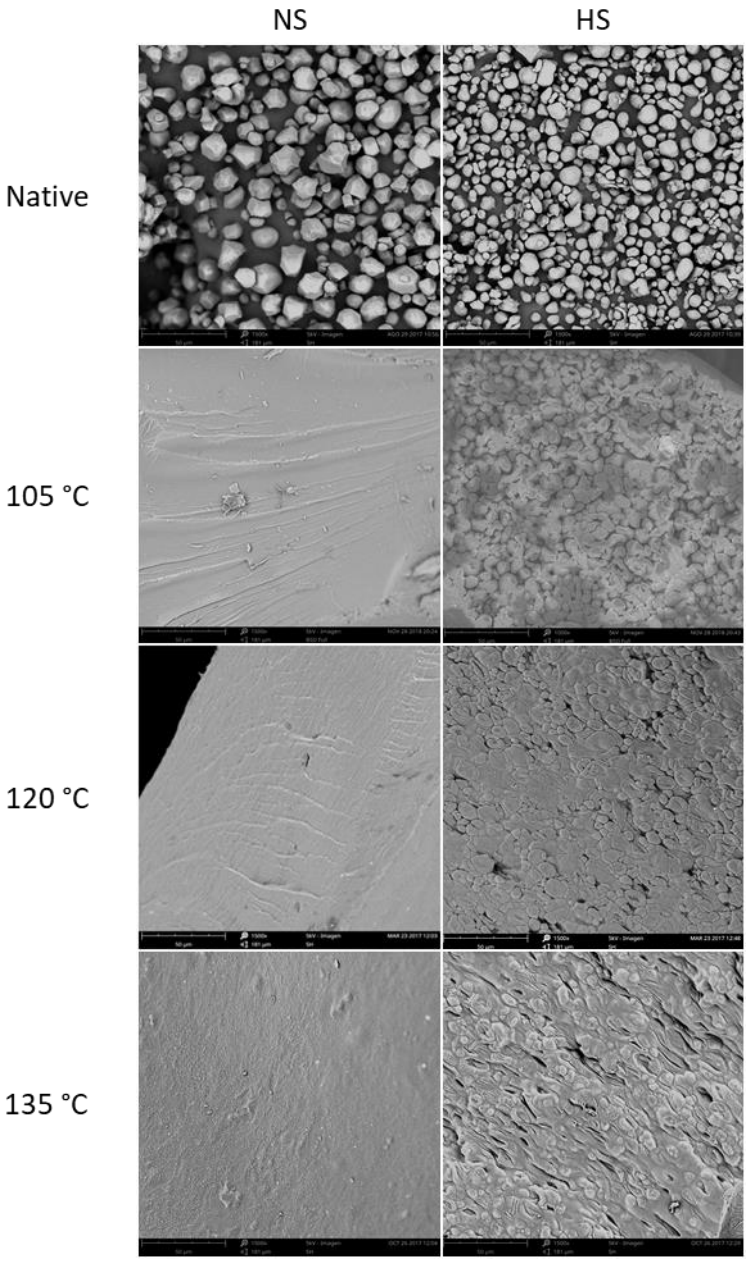

Figure 17 - SEM images of native and autoclaved starches at different temperatures

The granules of NS were essentially large and polygonal as reported by Lin et al. (2016). The autoclaving process caused remarkable changes in the granular morphology, even at 105 °C. From micrographs, the starch granules practically disappeared and the aggregation of the molecular components led to the formation of an irregular structural matrix at 105 °C, which became more homogeneous at 120 and 135 °C.

HS had spherical, irregular, and elongated granules with heterogeneous sizes. Similar findings have been described by Chen et al. (2017b) and Yang et al. (2016). As expected, the HS granules showed great resistance to autoclaving due to their high amylose content. At 105 °C, the starch granules adhered, and the large granules showed superficial indentations. After autoclaving at 120 °C, the granules were deformed and the indentations in the large granules became more visible. The indentations are due to the collapse of the granule inner region in which it is considered that the gelatinization begins (Chen et al., 2017b). At 135 °C, the large granules gelatinized, and the small granules were incompletely gelatinized. The high resistance to gelatinization of small granules is attributed to their higher content of amylose and amylopectin long branch-chains, lower content of amylopectin short branch-chains, and smaller branching degrees than that in large granules (Chen et al., 2017b; Peymanpour et al., 2016).

The morphological modifications observed in NS and HS granules could be explained by swelling, leaching of granular components, a complete (NS) or partial (HS) disruption of the granular structure resulting from the autoclaving process, and the subsequent reorganization of the starch chains during recrystallization.

5.3 CRYSTALLINE STRUCTURE

The XRD patterns of native and autoclaved starches are shown in Figure 18.

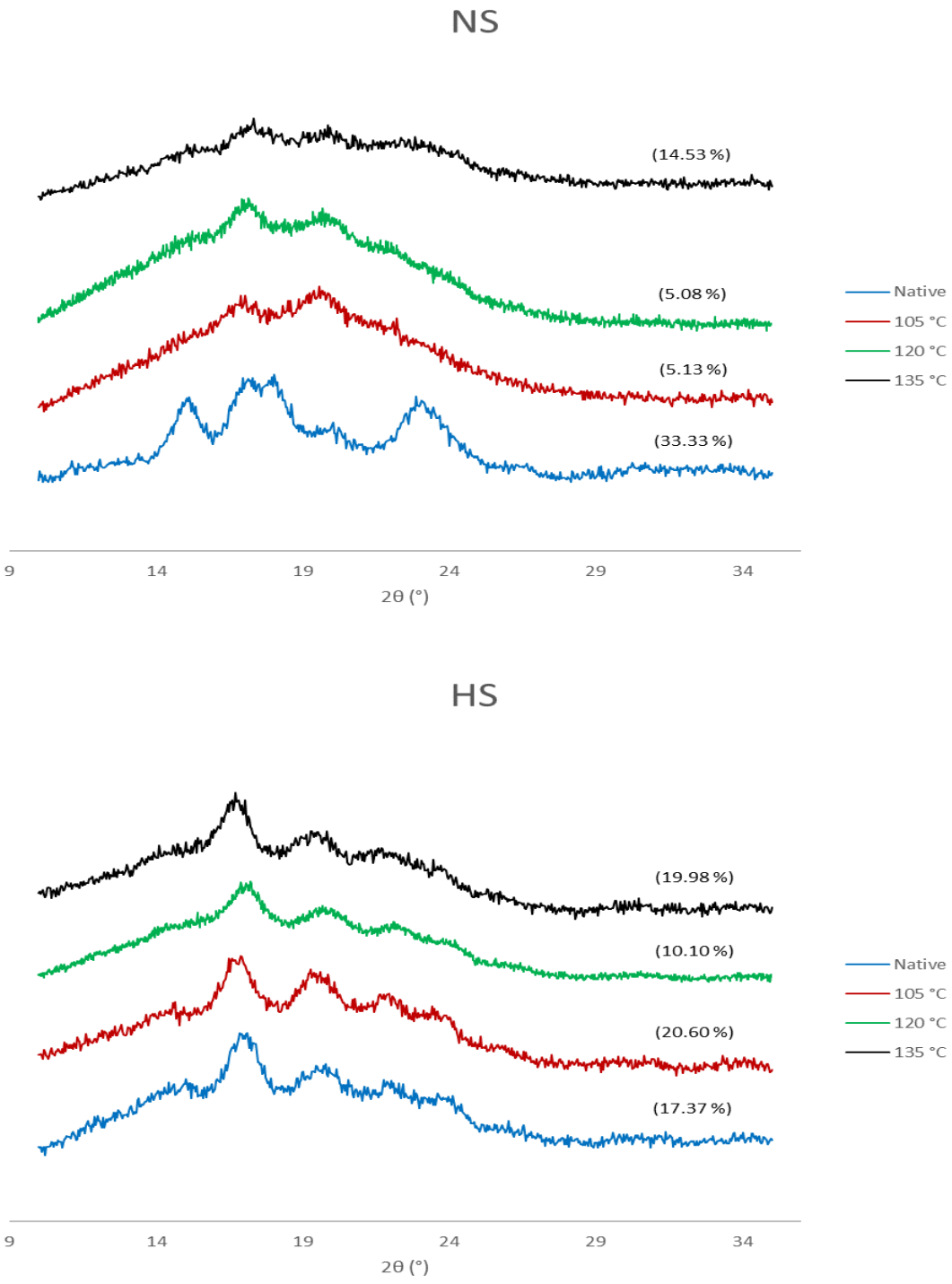

Figure 18 - X-ray diffractograms of native and autoclaved starches at different temperatures. The RC is presented in brackets

NS showed the A-type pattern, with strong reflections of 2θ at around 15° and 23°, and an unresolved doublet at 17° and 18°, as reported by Lin et al. (2016). The autoclaving treatment resulted in starches with B-type pattern showing reflections of 2θ at around 15°, 17°, 20°, 22°, and 24°. The transition from A-type to B-type pattern revealed that the autoclaving process disrupted completely the crystalline structure of NS (Guo, Yu, Copeland, Wang, & Wang, 2018). On the other hand, HS showed a B-type pattern, typical of high amylose starches (Lin et al., 2016). The autoclaving treatment did not change the XRD pattern; however, the intensity of the diffraction peaks changed, indicating rearrangements of the crystalline structure.

The change of RC for both starches after the autoclaving process is shown in Figure 18. The RC of NS (33.33%) decreased after the treatment, reaching the highest value at 135 °C (14.53%). The RC decrement of NS indicates that the crystalline structure of the granules, which is mainly conformed by double-helical crystallites of amylopectin adjacent linear chain segments (Pérez & Bertoft, 2010) had a lower resistance to the autoclaving treatment. Autoclaving supplied enough energy that in combination with the high content of water, promoted a cooperative process of gelatinization resulting in the melting of the double-helical crystallites of NS (Matignon & Tecante, 2017; Wang et al., 2015), overriding the hydrogen bonding and van der Waals forces that stabilize them (Imberty, Buléon, Tran, & Péerez, 1991). Moreover, after autoclaving, the gelatinized starch chains were organized in a less crystalline structure.

Regard to HS, the RC of the native sample (17.37%) increased after autoclaving at 105 ºC (20.60%). It is considered that the granular periphery of high amylose starch is constituted by amylopectin and amylose double-helical crystallites intertwined with amylose molecules while the granule inner region is the most crystalline, but also the most loosely packed region

(Yang et al., 2016). The increase of RC after autoclaving at 105 ºC could be attributed to the crystallization of amorphous amylose leached from the granules after the start of the gelatinization in the inner region (Chen et al., 2017b). With further increase in temperature (120 ºC), autoclaving disrupted the granule inner region decreasing the overall crystalline portion of HS (RC = 10.10%), as observed by SEM (Figure 17). The greater extent in the disruption of the granular structure reached after autoclaving at 135 °C resulted in a high amount of double helices packed in crystalline arrays (RC = 19.98%) after retrogradation (Pu, Chen, Li, & Li, 2013). The release of the amylose from the most thermally-resistant region of the granule along with the collapse of the inner region could have increased the availability of the starch chains to form more crystalline arrays.

5.4 DEGREE OF DOUBLE HELIX AND ORDER

The FTIR spectra of native and autoclaved starches are shown in Figure 19.

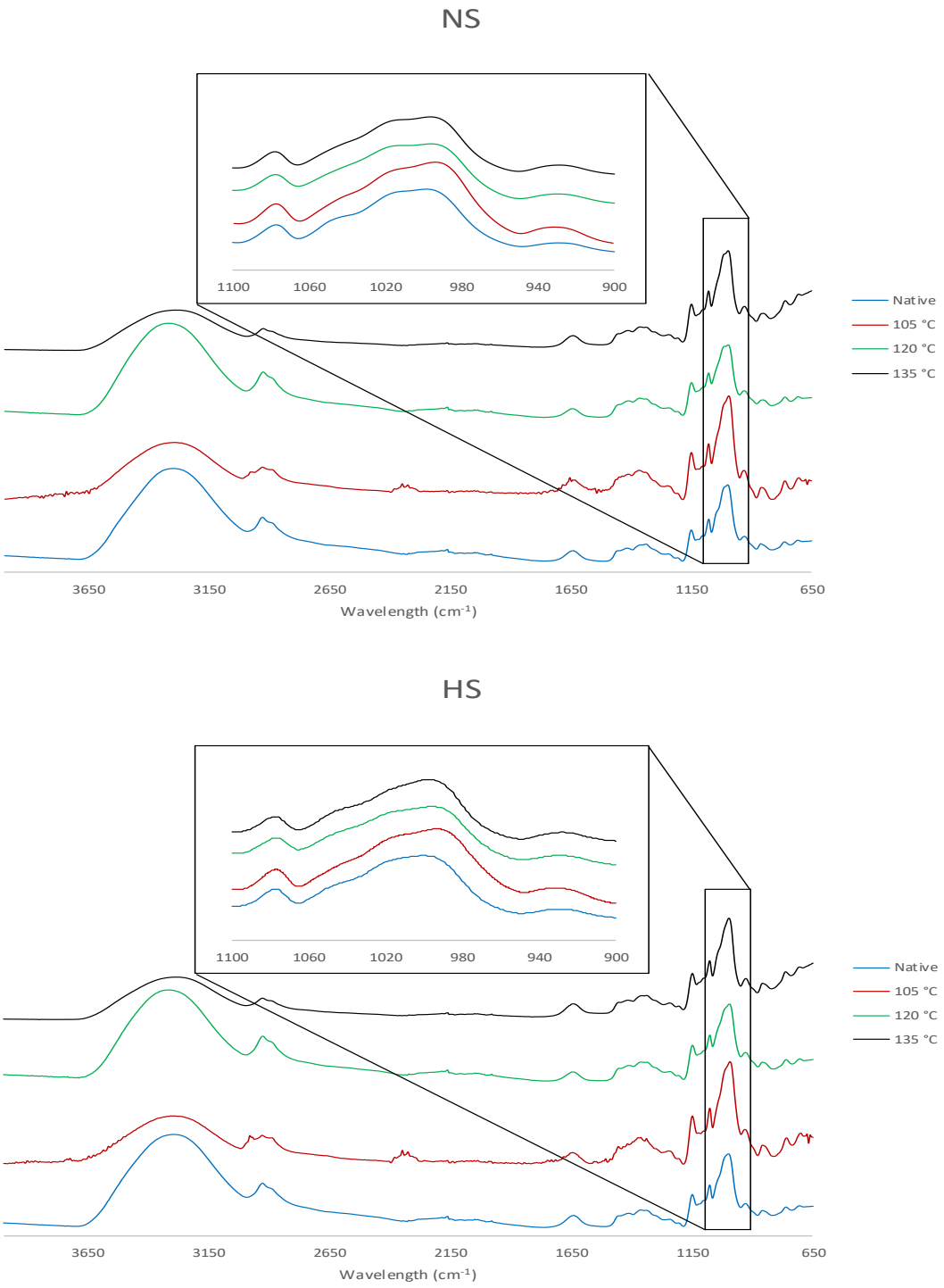

Figure 19 - FTIR spectra of native and autoclaved starches at different temperatures

The intensities of the peaks between 1100 and 900 cm^{-1} were different for native and autoclaved starches reflecting modification of the ordered region (995 and 1047 cm^{-1}) and the amorphous phase (1022 cm^{-1}) (Xu et al., 2019).

The ratios of the absorption band at 995/1022 cm^{-1} and 1047/1022 cm^{-1} are used to measure the variations in the degree of the double helix (DD) and degree of order (DO), respectively (Ma et al., 2018; Xu et al., 2019). The DD and DO of native and autoclaved starches are shown in Table 7.

Table 7 - DD and DO of native and autoclaved starches

Sample	DD (995/1022 cm^{-1})	DO (1047/1022 cm^{-1})
	NS	
Native	1.1027	0.7441
105 °C	1.1775	0.7182
120 °C	1.0671	0.7432
135 °C	1.0956	0.6642
	HS	
Native	1.0864	0.7349
105 °C	1.1763	0.6631
120 °C	1.1079	0.7547
135 °C	1.1742	0.7689

The DD value of NS (1.1027) increased after autoclaving at 105 °C (1.1775) but decreased at higher temperatures. The treatment at 105 °C disrupted the granular structure promoting a better alignment of the molecular chains to evolve towards a coil-to-helix transition during recrystallization, increasing the content of double helices (Ma et al., 2018). However, a more

intense treatment (120 and 135 °C) resulted in the disassociation of the double-helical structure. The autoclaving treatment decreased the DO value of NS, with the lowest value at 135 °C. This trend indicates that autoclaving reduced the compaction between double helices (Zhou et al., 2019). These results reveal that autoclaving not only resulted in the destruction of hydrogen bonds between adjacent double helices collapsing the crystalline structure of NS following the RC values (Figure 18) (Xu et al., 2019; Yin et al., 2018), but also in the disassociation of the double-helical structure under extreme temperature conditions.

The autoclaving process affected the DD of HS differently, increasing the values, from 1.1079 at 120 °C to 1.1763 at 105 °C. This behavior indicates that the autoclaving treatment allowed increasing the content of double helices, instead of disassociating the double-helical structure. On the other hand, the DO value of HS decreased after autoclaving at 105 °C but increased at higher temperatures, reaching a maximum value at 135 °C (0.7689). Opposite to NS, in HS the autoclaving process extended the double-helical structure probably through the cleavage of starch chains in the crystalline/amorphous region, which increased the mobility of the molecular chains favoring the arrangement of double helices (Xu et al., 2019). Also, the increased mobility of the molecular chains could have promoted a better alignment of the double helices at 120 and 135 ºC, increasing the compaction and favoring the DO values.

5.5 THERMAL PROPERTIES

The thermal parameters of native and autoclaved starches are shown in Table 8.

Table 8 - Thermal parameters of native and autoclaved starches

Sample	T_o (°C)	T_p (°C)	T_e (°C)	ΔT (°C)	ΔH (J/g)
			NS		
Native	$154.0^{c} \pm 4.1$	$155.0^{b} \pm 5.2$	$172.4^{c} \pm 5.0$	$18.4^{b} \pm 0.8$	$153.8^{a} \pm 4.0$
105 °C	$159.8^{b} \pm 1.6$	$160.8^{b} \pm 1.8$	$185.6^{b} \pm 2.4$	$25.7^{a} \pm 4.0$	$91.2^{c} \pm 3.7$
120 °C	$170.5^{a} \pm 1.4$	$171.4^{a} \pm 1.0$	$193.6^{a} \pm 0.7$	$23.1^{a} \pm 0.9$	$79.8^{d} \pm 6.8$
135 °C	$157.0^{bc} \pm 2.8$	$159.6^{b} \pm 3.5$	$182.7^{b} \pm 3.7$	$25.7^{a} \pm 0.9$	$107.5^{b} \pm 5.2$
			HS		
Native	$158.5^{b} \pm 1.5$	$160.3^{b} \pm 2.0$	$171.5^{c} \pm 1.9$	$13.0^{c} \pm 0.3$	$138.7^{b} \pm 2.2$
105 °C	$155.7^{b} \pm 3.1$	$159.2^{b} \pm 4.2$	$179.1^{b} \pm 3.7$	$23.3^{ab} \pm 0.5$	$103.6^{c} \pm 2.7$
120 °C	$169.4^{a} \pm 2.1$	$171.3^{a} \pm 1.2$	$193.5^{a} \pm 1.8$	$24.1^{a} \pm 2.6$	$85.1^{d} \pm 9.1$
135 °C	$151.0^{c} \pm 0.2$	$151.2^{c} \pm 0.2$	$176.8^{b} \pm 0.3$	$25.7^{a} \pm 0.0$	$143.2^{a} \pm 0.3$

For each starch, means with different letters in the same column are significantly different ($P < 0.05$).

An endothermic transition between 150 and 195 °C, which corresponds to the disorganization of the crystallites and double helices (Zhou et al., 2014) was observed for both starches. In general, the T_o, T_p and especially the T_e parameters of NS increased after the autoclaving process, reaching maximum values (T_o = 170.5 °C, T_p = 171.4 °C and T_e = 193.6 °C) at 120 °C. This increase suggested the formation of new double-helical crystallites with higher thermal stability, maybe resulting from stronger interactions of amylopectin-amylose or amylose-amylose promoted by the autoclaving treatment through disruption of the granular structure (Pratiwi et al., 2018).

On the other hand, in HS the autoclaving treatment at 105 °C did not change significantly the T_o and T_p. After autoclaving at 120 °C, those parameters increased (T_o = 169.4 °C and T_p = 171.3 °C), while at 135 °C decreased. Interestingly, the autoclaving process increased the T_e reaching a maximum value (193.5 °C) at 120 °C. Our results suggested that the autoclaving process could have affected the intensity of the intra or inter associations between amylose and amylopectin existing in native granules of HS, promoting the formation of double-helical crystallites with variable stability.

The hypothesis about the reason of the changes of transition temperatures is consistent with the ΔT (T_e-T_o) increase observed in both starches after the autoclaving treatment, which indicates that autoclaving resulted in the formation of crystallites and double helices with more heterogeneous structure than those of native starches (Wang & Copeland, 2015). During the storage of gelatinized starch, amylose and amylopectin associations occur, involving a recrystallization process (Lian et al., 2018).

The autoclaving process decreased the ΔH in NS, reflecting a lower degree of structural order in modified starches (Xu et al., 2019; Zhou et al., 2019), while in HS a similar behavior was observed, except at 135 °C, probably because of the formation of a highly ordered structural matrix, taking into consideration the content of double helices and their compaction (Table 7 - 1.1742 in DD and 0.7689 in DO), and the extent of the crystalline regions (Figure 18 - 19.98% in RC). Because of these trends in our results, ΔH can be used as an indicator of the structural ordering in starch (Warren et al., 2016).

5.6 WATER SOLUBILITY INDEX (WSI) AND SWELLING POWER (SP)

The WSI of native and autoclaved starches is shown in Figure 20.

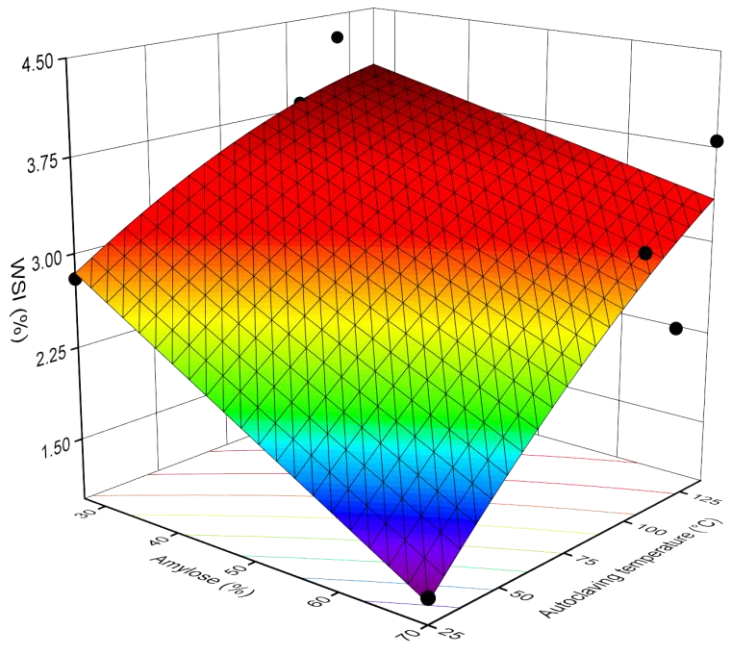

Figure 20 – WSI of native and autoclaved starches

The WSI of NS was higher than that of HS, reflecting its low resistance to thermal treatment, which led to the leaching of more starch molecules from the granules. The autoclaving treatment increased the WSI in both starches, with slight differences observed by the variation of the autoclaving temperature. The WSI of NS increased from 2.8% to 4.3% after the autoclaving treatment (120 °C), while in HS, the WSI increased from 1.2% to 3.8% after the modification (135 °C).

The SP of native and autoclaved starches is shown in Figure 21.

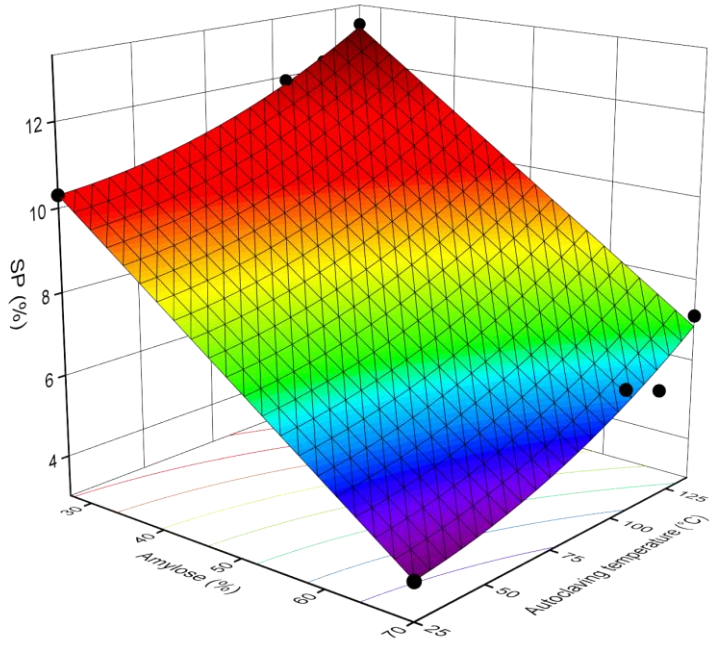

Figure 21 – SP of native and autoclaved starches

The autoclaving treatment increased the SP of both starches; however, no differences were found between 105 and 120 °C. The SP of NS and HS increased from 10.3% to 13.0% and from 3.9% to 7.1% after autoclaving, respectively.

5.7 WATER HOLDING CAPACITY (WHC) AND OIL HOLDING CAPACITY (OHC)

The WHC of native and autoclaved starches is shown in Figure 22.

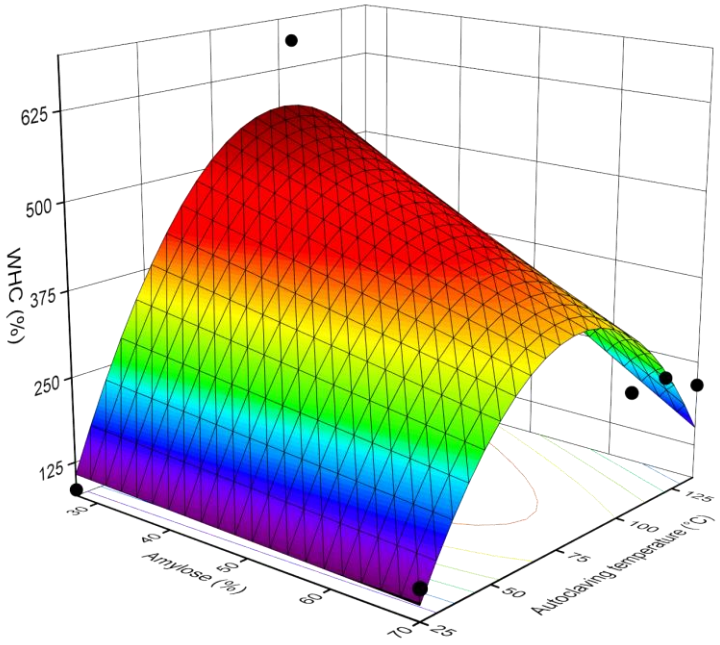

Figure 22 – WHC of native and autoclaved starches

The WHC was lower in NS (83.6%), maybe due to its A-type crystalline structure, high crystallinity (RC = 33.33%) and high amount of double helices (DD = 1.1027) more compact packed (DO = 0.7441). This more ordered structure could make it difficult for the water uptake (Fonseca-Florido et al., 2016). In contrast, HS has a B-type crystalline structure, RC of 17.37%, and lower content of double helices (DD = 1.0864) less densely packed (DO = 0.7349), which is related to a more disordered structure that could facilitate the water uptake (WHC = 119.2%).

The capacity of both starches to hold water increased after autoclaving, reaching the highest values after the treatment of the starches at 105 °C. The WHC of NS and HS increased from 83.6% to 665.0% and from 119.2% to 249.2% after the modification, respectively.

The OHC of native and autoclaved starches is shown in Figure 23.

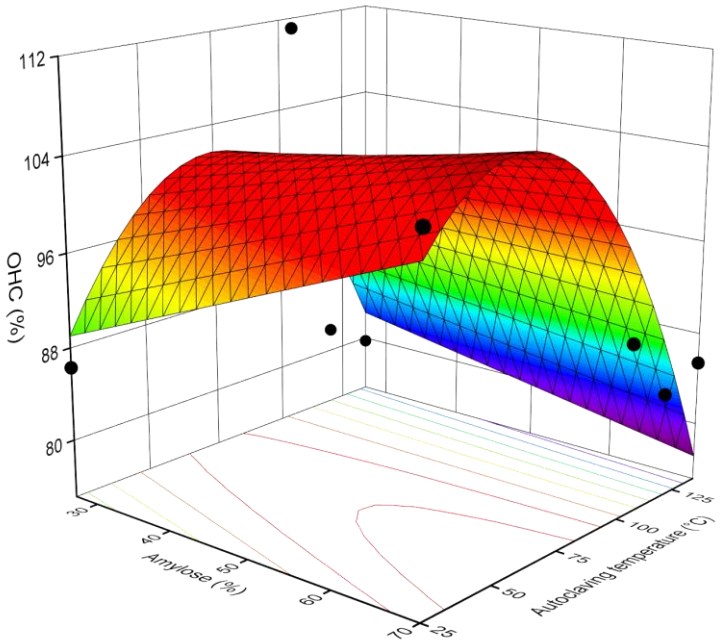

Figure 23 – OHC of native and autoclaved starches

After the autoclaving treatment, the OHC of both starches was modified. The OHC of NS increased from 86.3% to 111.1% after autoclaving at 105 °C but decreased after autoclaving at 120 (82.0%) and 135 °C (79.7%). On the other hand, the OHC of HS decreased from 104.4% to 83.9% after the autoclaving treatment (120 °C). As in NS, the increase of the autoclaving temperature reduced the OHC of the modified HS, and no differences were found at 120 and 135 °C.

5.8 RESISTANT STARCH (RS)

The RS content of native and autoclaved starches is shown in Figure 24.

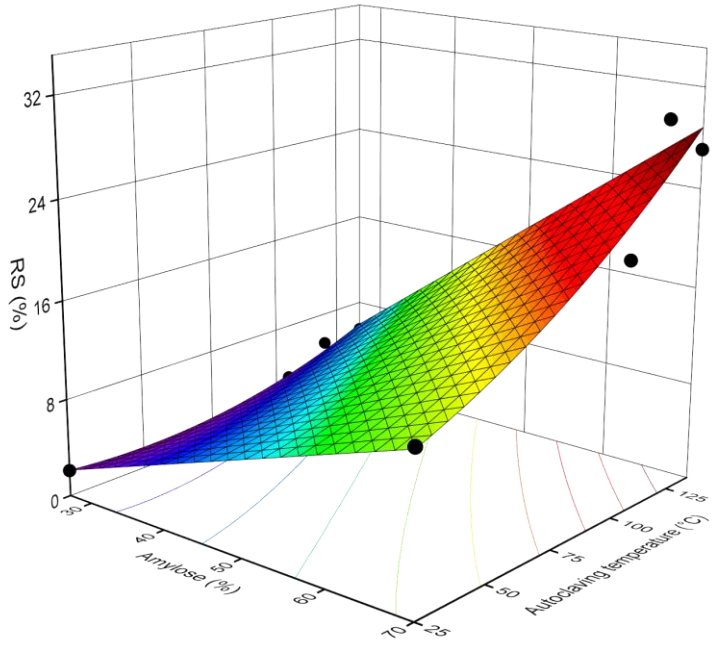

Figure 24 – RS of native and autoclaved starches

Compared to NS, HS was more resistant to enzymatic digestion, as confirmed by a higher RS content. The autoclaving treatment increased the RS content in both starches, ranging from 3.3 to 5.5% and from 20.2 to 30.2% in NS and HS, respectively. The physical modification of the granular structure by the autoclaving process increased the RS content. In autoclaved samples, the RS type 3 (RS3), which is a retrograded starch, is considered as the main fraction that contributes to the resistance to enzymatic digestion. HS showed more significant changes, reaching a maximum value of 30.2% at 120 °C.

5.9 FUNCTIONAL PROPERTIES RELATED TO STRUCTURE OF AUTOCLAVED STARCHES

To identify the relationship between the functional properties and the structural features of native and autoclaved starches, a correlation analysis was conducted. The analysis was segmented by starches. Table 9 and Table 10 correspond to NS meanwhile Table 11 and Table 12 correspond to HS. The first Table for each starch shows the results of the correlation analysis that was performed including the native and modified starches. In the second Table, the results of the analysis performed only with the modified starches are shown. In the next sections, the relationships will be discussed.

Table 9 - Correlation matrix between the data on functional properties and the structural parameters of native and modified NS

	WSI	SP	WHC	OHC	RS
RC	-0.94	-0.73	-0.97	-0.33	-0.63
DD	0.03	-0.05	0.56	0.99	-0.40
DO	-0.14	-0.75	-0.15	0.35	-0.61
T_o	0.87	0.39	0.55	-0.11	0.58
T_p	0.91	0.48	0.57	-0.17	0.67
T_e	0.99	0.67	0.80	0.03	0.73
ΔT	0.70	0.89	0.88	0.30	0.65
ΔH	-0.98	-0.74	-0.92	-0.21	-0.70

Table 10 - Correlation matrix between the data on functional properties and the structural parameters of modified NS

	WSI	SP	WHC	OHC	RS
RC	-0.63	0.96	-0.78	-0.55	0.56
DD	-0.44	-0.65	0.90	0.99	-0.98
DO	0.70	-0.94	0.72	0.48	-0.49
T_o	1.00	-0.44	0.05	-0.26	0.24
T_p	1.00	-0.34	-0.06	-0.36	0.34
T_e	0.99	-0.49	0.11	-0.20	0.18
ΔT	-0.99	0.25	0.15	0.44	-0.42
ΔH	-0.89	0.77	-0.46	-0.17	0.18

Table 11 - Correlation matrix between the data on functional properties and the structural parameters of native and modified HS

	WSI	SP	WHC	OHC	RS
RC	0.39	0.28	-0.16	0.24	-0.45
DD	0.86	0.81	0.85	-0.72	0.46
DO	0.12	0.23	-0.22	-0.18	0.41
T_o	-0.49	-0.40	0.19	-0.14	0.30
T_p	-0.50	-0.43	0.22	-0.11	0.23
T_e	0.16	0.25	0.72	-0.72	0.79
ΔT	0.90	0.93	0.91	-0.98	0.87
ΔH	0.01	-0.03	-0.69	0.50	-0.46

Table 12 - Correlation matrix between the data on functional properties and the structural parameters of modified HS

	WSI	SP	WHC	OHC	RS
RC	0.84	0.67	-0.43	0.74	-0.77
DD	0.45	0.21	0.07	0.98	-0.98
DO	0.29	0.53	-0.74	-0.85	0.82
T_o	-0.96	-0.86	0.68	-0.51	0.55
T_p	-0.99	-0.93	0.79	-0.37	0.41
T_e	-0.92	-0.79	0.59	-0.61	0.64
ΔT	0.65	0.83	-0.95	-0.56	0.52
ΔH	0.98	1.00	-0.94	0.05	-0.10

5.9.1 Water solubility index (WSI) and swelling power (SP)

According to Table 9, after the modification of NS, the WSI was positively correlated with T_o, T_p, T_e, and ΔT with r values of 0.87, 0.91, 0.99, and 0.70, respectively. In modified starches, the WSI was positively correlated to DO, T_o, T_p, and T_e, with r values of 0.70, 1.00, 1.00, and 0.99, respectively (Table 10). On the other hand, in HS, the WSI was positively correlated to DD and ΔT with r values of 0.86 and 0.90, respectively, after autoclaving (Table 11). In modified HS, the WSI was positively correlated to RC, ΔT, and ΔH with r values of 0.84, 0.65, and 0.98, respectively (Table 12).

The correlations suggest that the increased WSI observed in both starches after the autoclaving process (Figure 20) could be related to structural changes in the starch molecules or an independent mechanism that led to the mobility of the starch components, promoting its leaching from the starch structural matrix (Jagannadham et al., 2017).

After autoclaving, the SP of NS was positively correlated to T_e and ΔT with r values of 0.67 and 0.89, respectively (Table 9), while in modified starches, the SP was positively correlated to RC and ΔH, with r values of 0.96 and 0.77, respectively (Table 10). In HS, SP was positively correlated to DD and ΔT with r values of 0.81 and 0.93, respectively, after autoclaving (Table 11). In modified HS, SP was positively correlated with RC, ΔT, and ΔH with r values of 0.67, 0.83, and 1.00, respectively (Table 12).

The results suggest that the more intense interactions of amylopectin-amylose or amylose-amylose that resulted from the autoclaving process, deducted by the DSC measurements, could have formed a stronger network or entanglements that entrap water and swell, increasing the SP of both starches (Figure 21). Moreover, the highest SP values were observed after autoclaving the starches at 135 °C, as the overall structural order of autoclaved starches, indicated by ΔH (Table 8), was improved.

5.9.2 Water holding capacity (WHC) and oil holding capacity (OHC)

From Table 9, it can be observed that after autoclaving, the WHC of NS was positively correlated to T_e and ΔT, with r values of 0.80 and 0.88, respectively. In the modified starches, the WHC was positively correlated to DD and DO with r values of 0.90 and 0.72, respectively (Table 10). In HS, the WHC was positively correlated to DD, T_e, and ΔT, with r values of 0.85, 0.72 and 0.91, respectively (Table 11) after autoclaving, while in modified starches the WHC was positively correlated to T_o and T_p with r values of 0.68 and 0.79, respectively (Table 12).

The correlations suggest that after the autoclaving process, the more intense interactions of amylopectin-amylose or amylose-amylose improved the capacity of NS and HS to hold water (Figure 22). For both starches, the lowest value of WHC was observed after autoclaving at

135 °C, probably due to the stronger structural order (higher ΔH values after the modification, Table 8) reached, which restricted the capacity to hold water.

The OHC of NS after autoclaving and in the modified starches was positively correlated to DD with an r value of 0.99 (Tables 9 and 10). In HS, no structural parameter was positively correlated to OHC after autoclaving (Table 11), whereas, in the modified starches, the OHC was positively correlated to RC and DD, with r values of 0.74 and 0.98, respectively (Table 12).

The correlations suggest that the OHC of native and modified starches could be related to their helical structure. From Figure 23, in general, the autoclaving process reduced the OHC of both starches may be due to the unavailability of helical structures suitable to form complexes with lipids. A reduction in the lipophilic nature of both starches was noticed with the increase in the autoclaving temperature, which leads to the hypothesis that a double-helical structure more densely packed or ordered (Table 7), together with more crystalline regions (Figure 18), could have worked as a barrier that restricts oil accessibility to helical structures, inhibiting the capacity to hold the oil.

5.9.3 Resistant starch (RS)

According to Table 9, in NS, the RS was positively correlated with T_p, T_e, and ΔT with r values of 0.67, 0.73, and 0.65, respectively after the modification. In HS, the RS was positively correlated with T_e and ΔT, with r values of 0.79 and 0.87, respectively after autoclaving, as shown in Table 11. In modified HS, the RS was positively correlated to DO and T_e, with r values of 0.82 and 0.64, respectively (Table 12).

The correlations observed suggest that the crystallite quality, related to the double helices length (Singh, Singh, Kaur, Sodhi, & Gill, 2003), which was improved (higher transition temperatures, Table 8) through stronger interactions of amylopectin-amylose or amylose-amylose, is the determining factor for the RS formation in NS and HS after autoclaving treatment (Figure 24). The crystallite quality determines the effectiveness of digestive enzymes to attack the starch molecular components, influencing the RS development after autoclaving. Moreover, in HS the double-helical order of the modified starches (Table 7), including the order of double helices located inside of the crystallites and those located outside of the crystalline register (Wang et al., 2015; Warren et al., 2016), affected its resistance to enzymatic digestion.

The higher RS contents of modified HS (Figure 24) are congruent with the widely accepted idea that amylose is the main molecular component of RS obtained during the reorganization of gelatinized starch (Raigond et al., 2015); however, since amylose can co-crystallize with amylopectin (Lian et al., 2018), the contribution of amylopectin to the RS formation needs to be further studied, especially considering the structural complexity (increased ΔT values after the modification, Table 8) of autoclaved starch systems.

5.10 CONCLUSIONS

The autoclaving treatment of NS and HS resulted in contrasting structural changes. The low resistance of NS to autoclaving was manifested through the loss of granular morphology, the transition from A-type to B-type XRD pattern, a decrease in the RC, the disassociation of the double-helical structure at 120 and 135 °C and the decrease of the double-helical order. In HS, autoclaving caused structural rearrangements that resulted in partial disruption of the granules without changing the XRD pattern, an increase of RC (except at 120 °C, because of the collapse of the granule inner region) and double-helical structure, a high double-helical order at 120 and 135 °C and the formation of double-helical crystallites with variable stability. Together with the structural changes resulting from autoclaving, in both starches, the WSI, SP, WHC, and RS were increased, whereas the OHC, in general, was decreased. In this study, the increase in the WSI, SP, WHC, and RS upon autoclaving, was related to the more intense interactions of amylopectin-amylose or amylose-amylose produced by the modification process. Moreover, the functionality of the autoclaved starches was governed by the overall structural order. We expect that the obtained results contribute to a better understanding of the structural factors that affect the functional properties of autoclaved starches, which could help to obtain modified starches with tailored structures that modulate the starch functionality when used as an ingredient.

CHAPTER 6. EFFECT OF WATER CONTENT ON RESISTANT STARCH FORMATION AND STRUCTURE OF RETROGRADED AUTOCLAVED CORN STARCH WITH DIFFERENT AMYLOSE CONTENT

6.1 INTRODUCTION

Usually, the thermal treatments are applied to starch granules to obtain suitable physical properties intended for specific industrial applications (Zhang et al., 2017); so, the gelatinization and retrogradation phenomena play a crucial role in the final functionality of the starch. During starch retrogradation, water acts as a solvent promoting the migration of starch molecules and contributing to recrystallization processes (Tian et al., 2012). In this way, the recrystallization of amylopectin is not observed at 90% water content in waxy and normal corn starches (Zhou, Wang, Yoo, & Lim, 2011), because the high content of water led to an increased migration rate of starch molecules (Tian, Li, Xu, & Jin, 2011). Moreover, at 70-80% of water content, the presence of amylose affects the recrystallization of amylopectin during retrogradation (Zhou et al., 2011). The effect of water on the structure of retrograded starch impacts its digestibility. The water content of 66.7% allowed obtaining a maximum yield of slowly digestible starch in recrystallized waxy rice starch (Tian et al., 2012), attributed to a balance between the required water for the migration rate and the necessary water for recrystallization of starch molecules (Tian et al., 2011). Hsu, Lu, Chang, & Chiang (2015) reported that the amount of added water had a significant effect on the digestibility of retrograded starch in cooked rice flour.

In the literature, the structural and digestibility behaviors of retrograded starch have been reported extensively; however, there is a lack of information about the effect of the structure of autoclave-gelatinized starch retrograded under controlled hydration conditions on the formation of RS, one of the most relevant aspects of the functionality of retrograded starch. In this chapter, the effect of water content on RS formation and structure of retrograded autoclaved corn starch with different amylose/amylopectin ratios will be discussed. NS and HS were autoclaved at 120 °C and labeled as ANS and AHS. Subsequently, ANS and AHS were retrograded under controlled hydration conditions at 20 °C for 7 days. The RS fraction of the retrograded starches was determined, and its structural changes were evaluated by DSC, XRD, and FTIR-ATR.

6.2 WATER CONTENT OF RETROGRADED STARCHES

The relationship between the water content of retrograded starches and water activity (Aw ≈ RHeq/100) is shown in the water adsorption isotherms (Figure 25).

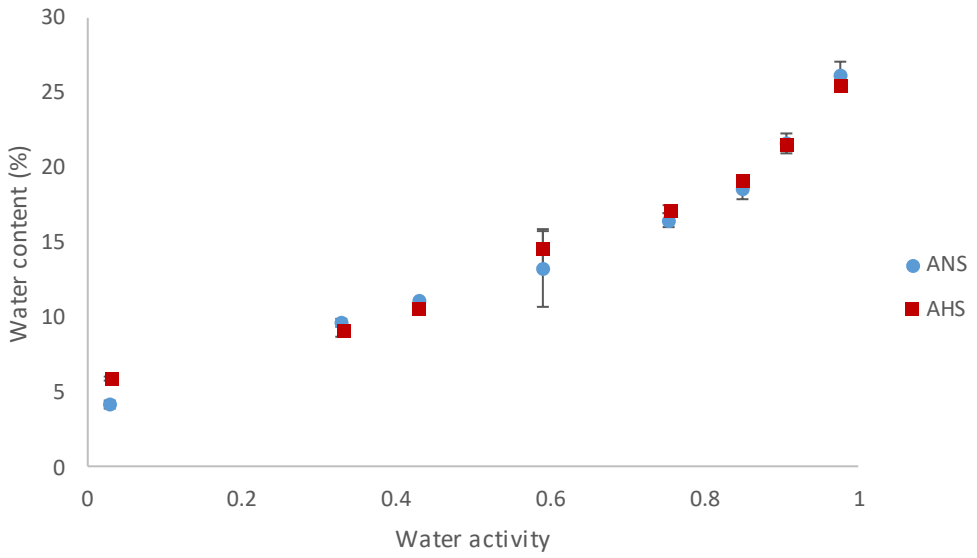

Figure 25 - Water adsorption isotherms of retrograded starches

The shape of the isotherms was similar for both starches. A slight increase in water content in the range from 0.3 to 0.6 of water activity was observed. At higher water activity values, the increase was exponential, reaching water content around 26% at a water activity of 0.97. From this, four water contents were selected to evaluate the effect on the RS formation and structure of autoclaved starches. The selected water contents were 4.20, 16.44, 21.60 and 26.22% for ANS and 5.92, 17.22, 21.61 and 25.52% for AHS, according to the water adsorption isotherms, corresponding to the equilibrium water content obtained at 0.03, 0.755, 0.906 and 0.976 Aw, respectively for each starch. The lower values selected (4.20 and 5.92%) were used as a reference when no water was added; at this condition, silica gel was used to obtain a dry environment. The other selected water contents were considered to be enough to promote the retrogradation of autoclaved starches during storage for 7 days at 20 °C.

6.3 RESISTANT STARCH (RS)

The RS content of retrograded starches after storage for 7 days is shown in Table 13.

Table 13 - RS content (g/100 g) in autoclaved corn starches retrograded at different water contents for 7 days at 20 °C

Water content (%)	RS (%)
ANS	
4.20	$5.1^{b} \pm 0.0$
16.44	$6.1^{a} \pm 0.3$
21.60	$6.6^{a} \pm 0.9$
26.22	$6.5^{a} \pm 0.3$
AHS	
5.92	$29.0^{c} \pm 2.8$
17.22	$34.2^{b} \pm 0.1$
21.61	$38.3^{a} \pm 1.0$
25.52	$38.8^{a} \pm 3.0$

For each starch, means with different letters are significantly different ($P < 0.05$).

The indigestible fraction of starch in the retrograded samples was affected by the water content. The RS content ranged from 5.1 to 6.6% and from 29.0 to 38.8% for ANS and AHS, respectively. The RS had the maximum values under hydration condition, reaching an increment of 29.41 and 33.79% for ANS and AHS, respectively. In ANS, the highest value of RS was observed at a water content of 21.60%; however, no significant differences were observed in the RS at the water content ranging from 16.44 to 26.22%. In AHS, the water content of 25.52% produced the highest RS amount; however, it was not significantly different from the amount obtained at a water content of 21.61%. As expected, compared to ANS, AHS presented a greater resistance to enzymatic digestion, as confirmed by the higher

contents of RS. To understand the digestibility changes, the retrograded starches were further investigated by DSC, XRD, and FTIR-ATR.

6.4 THERMAL PROPERTIES OF RETROGRADED STARCHES

In the thermal analysis after 7 days of storage under the RHeq environments, ANS showed two endothermic transitions, while AHS showed only one (Figure 26).

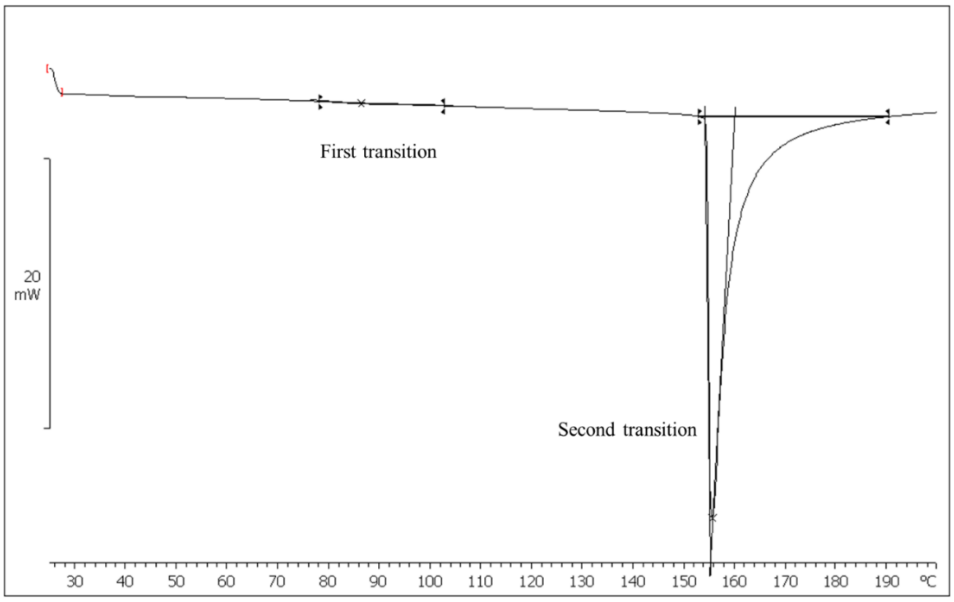

Figure 26 – Endothermic transitions observed in retrograded starches. The sample presented in the image is the ANS retrograded at 26.22% of water content

The first transition for ANS (Table 14) is related to the melting of the recrystallized side chains of amylopectin, which generally takes place at T_p values between 55 and 70 °C (Eerlingen & Delcour, 1995).

Table 14 - Thermal properties for recrystallized side chains of amylopectin

Water content (%)	T_o (°C)	T_p (°C)	T_e (°C)	ΔH (J/g)
4.20	ND	ND	ND	ND
16.44	$95.8^{a} \pm 3.7$	$104.0^{a} \pm 5.3$	$115.8^{a} \pm 7.2$	$0.3^{c} \pm 0.0$
21.60	$85.9^{b} \pm 4.7$	$95.9^{ab} \pm 5.5$	$105.5^{ab} \pm 5.3$	$0.5^{b} \pm 0.0$
26.22	$81.0^{b} \pm 2.5$	$89.9^{b} \pm 3.1$	$104.2^{b} \pm 1.1$	$1.1^{a} \pm 0.1$

Means with different letters in the same column are significantly different ($P < 0.05$). ND: Not detected.

However, the T_p values for the melting of the recrystallized amylopectin chains in this study (89.9-104.0 ºC) were higher than those values reported by other authors. This behavior could be attributed to the high disorganization extent of native starch reached during the thermal treatment in the autoclave (Figure 17). Trinh (2015) reported T_p values for recrystallized amylopectin between 68.1 and 95.1 °C for starches autoclaved at 120 °C. No melting signal for the recrystallized amylopectin was detected at the lowest water content, suggesting that its reorganization is limited by the water availability and the storage time as these measurements were carried out after storage for 7 days at 20 °C. The transition temperatures decreased when the water content increased; meanwhile, the ΔH values increased up to 0.3, 0.5, and 1.1 J/g for 16.44, 21.60 and 26.22% water content, respectively, indicating a higher structural order in the amylopectin component of ANS as the water content increased.

The second endothermic transition was observed around 150 °C and it corresponds to the melting of amylose crystallites (Eerlingen & Delcour, 1995; Trinh, 2015) (Figure 27).

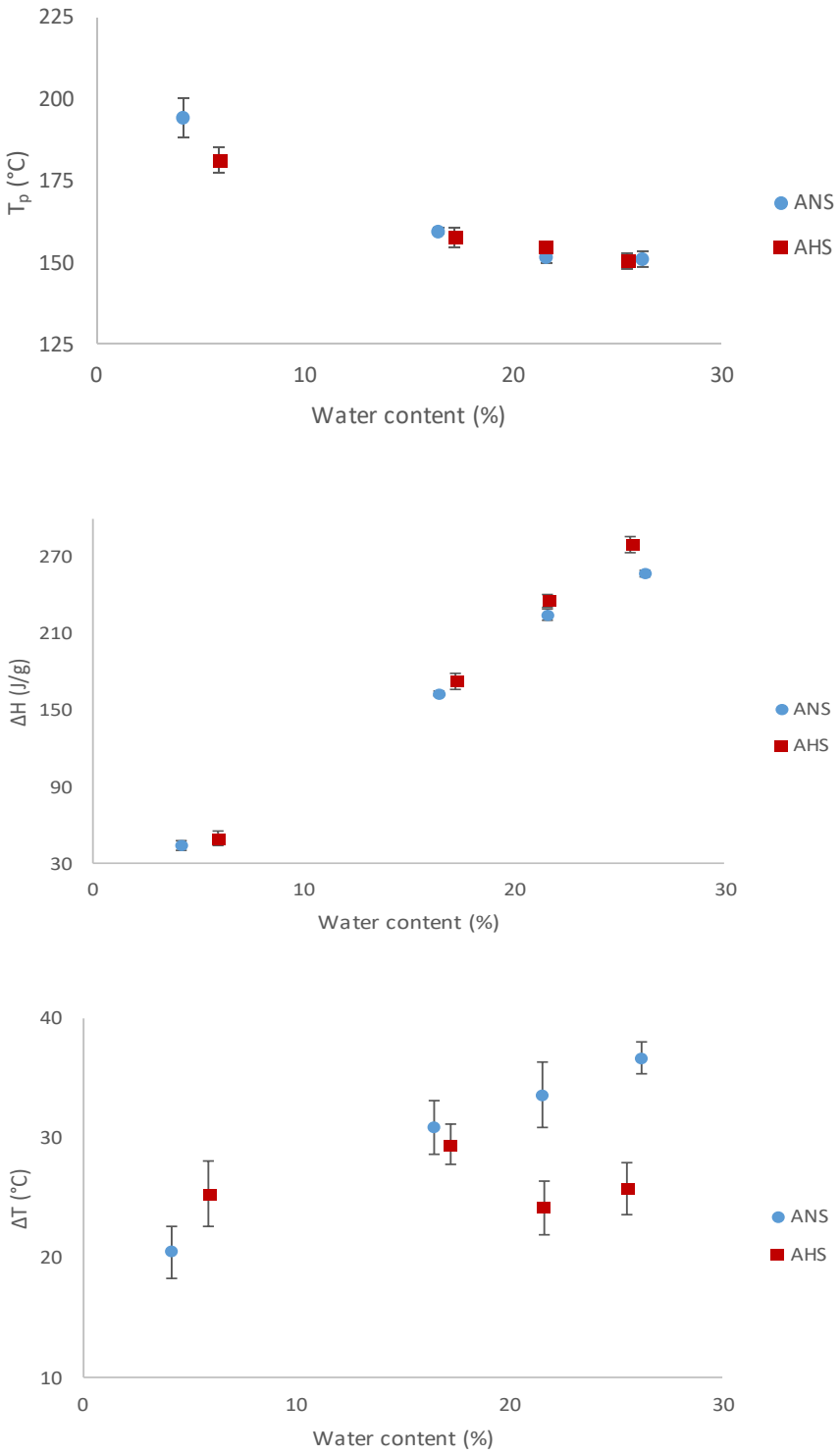

Figure 27 - Effect of water content on (upper) T_p, (middle) ΔH and (bottom) ΔT of amylose crystallites in retrograded starches

The transition temperature (T_p – Figure 27, upper section) decreased as the water content increased for both starches; meanwhile, the ΔH values, which are shown in Figure 27, middle section, increased from 44.2 to 257.2 J/g for ANS and from 50.0 to 280.5 J/g for AHS. The highest values were detected at water contents of 26.22 and 25.52%, respectively.

The decreasing of the transition temperatures and the increase of ΔH for melting of amylopectin and amylose when the water content increased in ANS and AHS can be attributed to the formation of a better-organized structure, but this was not reflected in an increment in RS content as shown previously (Table 13). Interestingly, the melting of amylose crystallites in AHS required a high amount of energy resulting in higher ΔH values. Also, the low ΔT (T_e-T_o) values (Figure 27, bottom section) in AHS suggest more homogeneous amylose crystallites, especially at high water contents. In the case of ANS, the ΔT values for the melting of amylose crystallites showed an increasing trend indicating the presence of heterogeneous crystallites with variable stability (Banchathanakij & Suphantharika, 2009). This result agrees with the increase in ΔH of recrystallized amylopectin (Table 14); therefore, the recrystallization of amylopectin could have prevented the formation of homogeneous amylose crystallites for ANS, because of this, higher values of ΔT for melting of amylose crystallites were found when compared with AHS. In granular starch, (Yang et al., 2016) suggested that the amorphous amylose acts as a diluent of amylopectin, responsible for the crystalline portion of the granule. In the present study, the opposite condition was found as the amylopectin chains could have acted as a diluent during the amylose rearrangement in ANS.

6.5 CRYSTALLINITY OF RETROGRADED STARCHES

To evaluate the effect of the water content on the crystallinity, the retrograded starches were analyzed using XRD. The X-ray diffractograms of ANS and AHS at different water contents are shown in Figure 28.

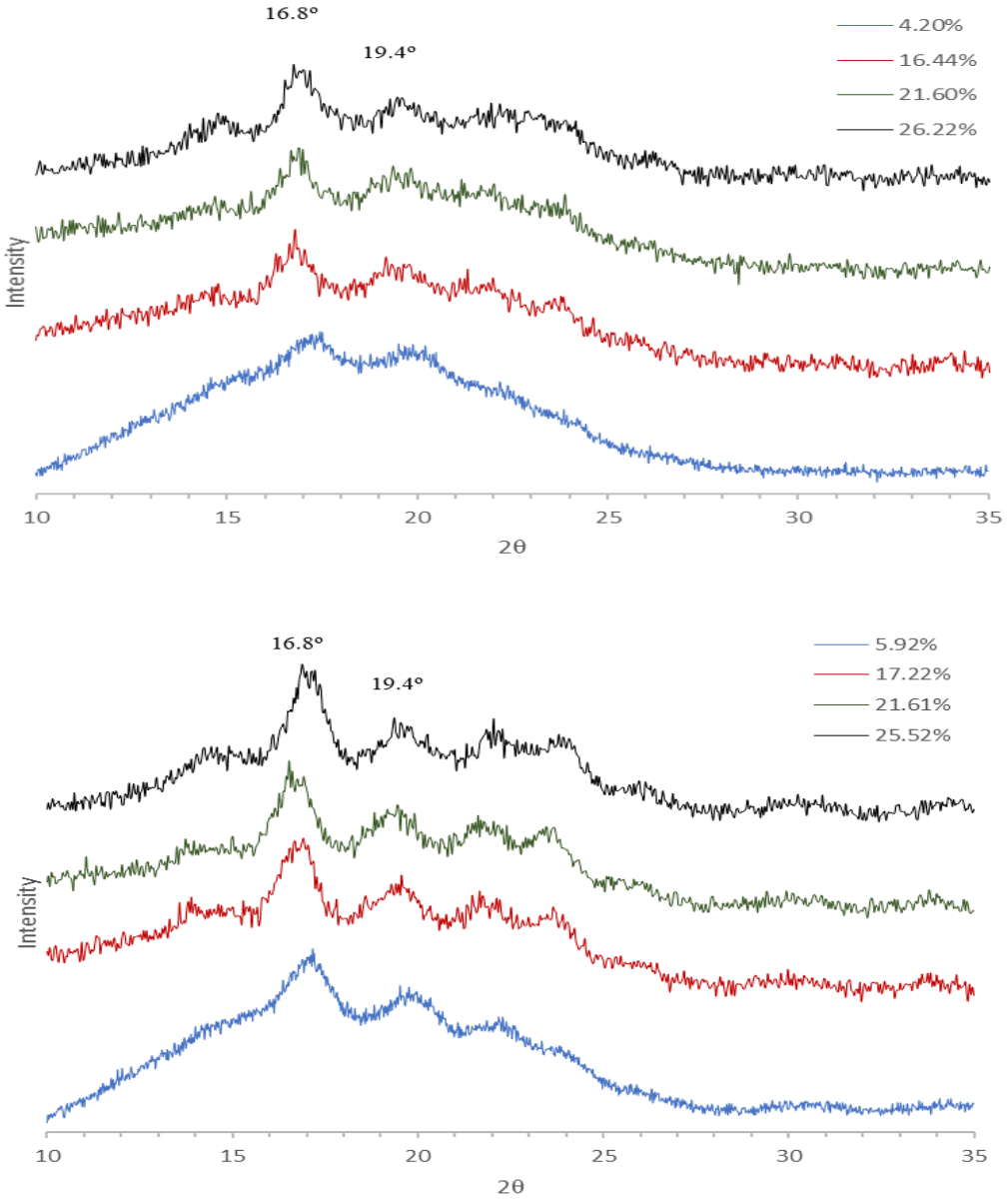

Figure 28 - X-ray diffractograms of (upper) ANS and (bottom) AHS retrograded at different water contents

The retrograded starches showed the B-type pattern after storing the autoclaved samples at 20 °C for 7 days. Kim, Choi, & Moon (2015) reported a B-type crystalline structure in gelatinized corn starch stored at low temperatures. Also, storing gelatinized starch at temperatures between 0 and 68 °C resulted in the formation of the B-type crystalline structure (Eerlingen & Delcour, 1995). In this study, the water content did not change the type of crystalline structure, but the intensity of the diffraction peaks increased when the water content increased, especially those at 16.8º and 19.4º; this trend was more noticeable for AHS.

The percentage of crystalline material (RC - Figure 29), which is formed by double helices arranged regularly and repeatedly in A- or B-type polymorph (Lopez-Rubio, Flanagan, Gilbert, & Gidley, 2008; Wang et al., 2015), increased in both starches when the water content increased.

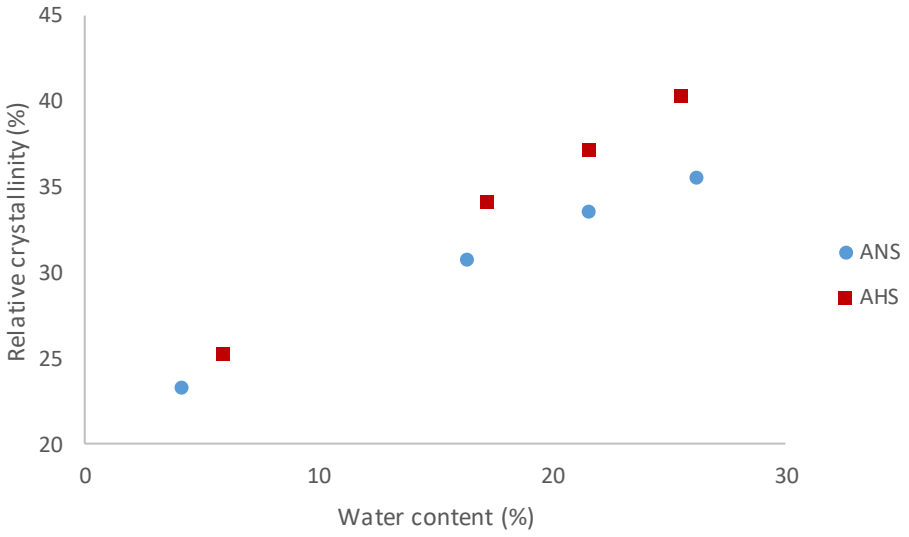

Figure 29 - Effect of water content on RC of retrograded starches

The maximum values of RC (35.52 and 40.35%) were reached for ANS and AHS, respectively at the highest water content. These results indicate that the formation of crystalline phases in the retrograded starches was promoted when the water content increased. This could be attributed to the increased mobility of amylose and amylopectin chains, which were rearranged forming more crystalline regions (Ding et al., 2019). Regardless of the water content, AHS showed higher values of RC, reflecting the easiness of amylose to form crystallites and entanglements due to its capability to interact through hydrogen bonds to a greater extent than the amylopectin molecules (Yang et al., 2016). Interestingly, even when the increased water content improved the crystalline structure of retrograded starches, the values of RS did not change in the same proportion (Table 13), suggesting that the increased crystallinity is not decisive for the RS formation in retrograded autoclaved starches.

6.6 DOUBLE HELICAL ORDER OF RETROGRADED STARCHES

The $R_{1000/1022}$ cm^{-1} (Figure 30) in the FTIR signal was used to measure the changes in the double-helical order of retrograded starches.

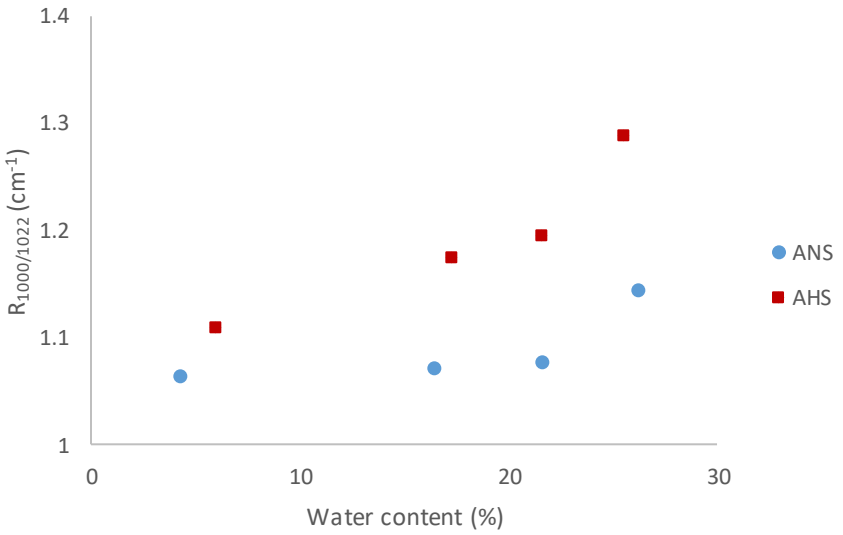

Figure 30 - Effect of water content on $R_{1000/1022}$ cm^{-1} of retrograded starches

This ratio increased in both starches as a function of the water content in a non-linear way. The increase of the $R_{1000/1022}$ cm^{-1} could be related to a better association of double helices or higher double-helical order (Capron et al., 2007). For ANS, the highest value was observed at the water content of 26.22% ($R_{1000/1022}$ cm^{-1} = 1.145). In AHS, the $R_{1000/1022}$ cm^{-1} reached the highest value at water content of 25.52% ($R_{1000/1022}$ cm^{-1} = 1.290). Both samples reached the highest values at the highest water content tested. In starch, the hydroxyl groups in the glucose units are adsorptive sites for binding water molecules through hydrogen bonds (Shittu, Idowu-Adebayo, Adedokun, & Alade, 2015). When the water content increased, the allocation of these bonds through the double helices promoted the inter-double-helices

conformation inducing significant modification on the polymeric chains in the whole matrix of retrograded starches.

The FTIR results suggest a plasticizing effect on the structural matrix of autoclaved starches, showing that the adsorbed water affected not only the amylopectin component but also the amylose. This behavior agrees with the endothermic transitions for amylopectin and amylose detected by DSC (Table 14 and Figure 27). In ANS, a slight increase in $R_{1000/1022}$ cm^{-1} was observed in the range from 4.20 to 21.60% of water content, reflecting low mobility for double helices alignment in a system with a high proportion of branched chains. In a structural matrix, composed mainly of long linear chains like in AHS, the $R_{1000/1022}$ cm^{-1} increased linearly with the water content in the 5.92-21.61% range, indicating high mobility of double helices for a better alignment. Moreover, the high values in $R_{1000/1022}$ cm^{-1} observed in AHS, indicate the capacity of double helices of amylose to form a more layered structure. According to Goodfellow & Wilson (1990), in retrograded systems, the amylopectin side chains can form double helices, which slowly get packed and stacked to form crystalline regions. Because of the branched nature of the amylopectin molecules, the helices formed are still connected to the main polymer chain; consequently, the range of energies for the main chain and the chain segments connecting the helical regions is high, decreasing the ordering of double helices. This effect is different for amylose molecules, where the aggregation of the helices results in disordered amorphous regions connecting the aggregated sections; so, the order of double helices of the system is not affected. The increased water content facilitated the mobility of double helices of amylopectin and amylose in autoclaved systems; however, the mobility degree depends on the molecular configuration, i.e., branched or linear nature, affecting the RS formation (Table 13) in retrograded ANS and AHS.

6.7 RESISTANT STARCH (RS) FORMATION IN RETROGRADED STARCHES

Based on the structural features of ANS and AHS previously discussed, we can propose a possible explanation about the formation of RS in autoclaved systems retrograded under controlled hydration. First, in ANS, an autoclaved system with an amylopectin/amylose ratio of 73/27%, our research suggests that the amylopectin recrystallization, promoted by the increased water content (Table 14), hindered the formation of RS. In AHS, the crystalline and double-helical order and the RS content were favored (not in the same proportion) with the increase in the degree of hydration. In ANS, only the crystalline and double-helical order were promoted and the RS content did not change in the range from 16.44 to 26.22% of water content. Therefore, the recrystallization of amylopectin in retrograded ANS could have inhibited the crystallization of amylose, the main component of the retrograded RS (Raigond et al., 2015). Also, the high values of crystallinity and the better alignment of double helices reached in the range from 21.61 to 25.52% of water content in retrograded AHS could be related to the increase of the resistance to enzymatic digestion; however, more research is needed to understand the mechanism of RS formation during the retrogradation of autoclaved starches under controlled hydration conditions.

6.8 CONCLUSIONS

This study showed the effect of water content provided by controlled hydration on the retrograded structure and RS formation in autoclaved corn starches with different amylopectin/amylose ratio. The storage at water content (~4-26%) acquired under controlled hydration resulted in remarkable changes in the structure of retrograded starches. The adsorbed water promoted the ordering of glucan chains in closed packed double helices and crystalline structures as confirmed by the high values of $R_{1000/1022}$ cm^{-1} and RC of ANS and AHS at the highest water contents. This trend was congruent with ΔH behavior. AHS showed a high degree of retrogradation as the water molecules promoted the mobilization of the linear chains of amylose, its main component. In ANS, the recrystallization of amylopectin, promoted by the increased water content, interfered with the formation of homogeneous double-helical crystallites of amylose preventing the formation of retrograded RS, reaching values around 6%. In AHS, the increase of the water content favored the amylose retrogradation, forming structures (double helices closely arranged and more crystalline regions) related to high values of RS. The information obtained from this work depicted the structural behavior of autoclaved corn starches retrograded under controlled hydration conditions and the repercussions on the RS formation, which enhance the understanding of the structural and nutraceutical properties of starch.

CHAPTER 7. GENERAL DISCUSSION AND CONCLUSIONS

The results showed that acid hydrolysis and autoclaving carried out under different times and temperatures, respectively, applied to different corn starches, NS, and HS, resulted in different changes at the structural level. The changes in the structure affected the functionality of both starches.

The acid hydrolysis caused a complete granular disruption accompanied by an increase in the double-helical structure of NS and HS. The double-helical order of the native starches decreased after the acid hydrolysis, except for HS hydrolyzed at 15 days. The increased acid hydrolysis time led to the formation of a more packed double-helical structure in both starches. The changes in the double-helical structure indicate the cleavage of the amylose chains located in the amorphous regions, which allowed the reorganization of the released chains into double helices. The ΔH behavior supports the degradation of the amorphous regions in NS. Also, although the acid showed a degrading effect on the double-helical order of the native starches, the extension of the hydrolysis time allowed the formation of shorter linear chains that compacted more efficiently or the reorganization of decoupled double helices.

Results indicate that the acid hydrolysis is a suitable modification process to improve the WSI and OHC of NS and HS. The WSI is a functional property resulting from the great degradative effect of the acid on the granular structure, also, the acid hydrolysis led to the formation of suitable helical structures for the interaction with the oil. Moreover, the information obtained about the effect of the acid hydrolysis time on the degradation of the amorphous regions and changes on the double-helical structure of NS and HS can be used to produce starch nanoparticles which have applications in a wide variety of industries such as pharmaceuticals, health care products, coloring substances, and biodegradable edible films.

The autoclaving process disrupted the granules, destroyed the hydrogen bonds between adjacent double helices collapsing the crystalline structure and, under severe temperature conditions, disassociated the double-helical structure of NS; whereas in HS, a partial granular disruption was observed, the crystalline structure was rearranged and the order of double-helical structure was improved at 120 and 135 °C. Despite the contrasting structural changes, the autoclaving treatment improved the quality of the double-helical crystallites in both starches which resulted from stronger interactions of amylopectin-amylose or amylose-amylose promoted by the granular disruption.

The autoclaving treatment can be an appropriate method to improve the SP and WHC of NS and HS. NS and HS modified by autoclaving have an enhanced water holding and swelling, derived from the more intense interactions between starch molecules. Also, autoclaving increased the RS content in both starches, through the improvement of the crystallite quality. In modified HS, the higher compaction density of the double helices increased the resistance to enzymatic digestion. Since RS is a starch fraction with relevant nutraceutical properties, its formation was further studied after a short-term retrogradation of the autoclaved starches, ANS and AHS, under controlled hydration conditions. The increased water content promoted the ordering of the starch chains in closed packed double-helices and crystalline structures in both starches. In AHS the RS content increased up to 38.8%, mainly due to the formation of homogeneous double-helical crystallites of amylose; whereas in ANS, the recrystallization of the amylopectin interfered with the formation of such crystallites, inhibiting the formation of RS.

In summary, the functionality of NS and HS can be improved through the modification of the native structure selecting the appropriate method and condition process. The results obtained from this work are important to manufacture novel starch materials with specific

functionality. Further, they are the basis for additional work to expand the knowledge about starch processing and functionality. The study could be expanded to more starch types and the systematic combination of both processes, the acid hydrolysis, and the autoclaving treatment.

This thesis was based on the following papers:

Published:

Soler, A., Mendez-Montealvo, G., Velazquez-Castillo, R., Hernández-Gama, R., Osorio-Diaz, P., & Velazquez, G. (2020). Effect of Crystalline and Double Helical Structures on the Resistant Fraction of Autoclaved Corn Starch with Different Amylose Content. *Starch – Stärke*.

Soler, A., Valenzuela-Díaz, E. D., Velazquez, G., Huerta-Ruelas, J. A., Morales-Sanchez, E., Hernandez-Gama, R., & Mendez-Montealvo, G. (2020). Double helical order and functional properties of acid-hydrolyzed maize starches with different amylose content. *Carbohydrate Research, 490*.

In preparation:

Soler, A., Velazquez, G., Velazquez-Castillo, R., Morales-Sanchez, E., Osorio-Diaz, P., & Mendez-Montealvo, G. - Effect of limited water content on resistant starch formation and structure of retrograded autoclaved corn starches with different amylose content.

Also, another product of the project was the co-direction of the following thesis:

Valenzuela-Díaz, E. (2019). *Efecto de la hidrólisis ácida en la morfología y en las propiedades funcionales de almidón de maíz* (Tesis de licenciatura). Tecnológico Nacional de México, Instituto Tecnológico de Acapulco, Guerrero, México.

BIBLIOGRAPHY

AACC. (2000). Approved methods of the American association of cereal chemists.

Ai, Y., & Jane, J. L. (2018). Understanding Starch Structure and Functionality. In *Starch in Food: Structure, Function and Applications: Second Edition* (pp. 151–178).

Amini Khoozani, A., Birch, J., & El-Din Ahmed Bekhit, A. (2019). Resistant Starch Preparation Methods. *Encyclopedia of Food Chemistry*, 390–394.

Ashwar, B. A., Gani, A., Wani, I. A., Shah, A., Masoodi, F. A., & Saxena, D. C. (2016). Production of resistant starch from rice by dual autoclaving-retrogradation treatment: Invitro digestibility, thermal and structural characterization. *Food Hydrocolloids*, *56*, 108–117.

ASTM (2012). E104-02 standard practice for maintaining constant relative humidity by means of aqueous solutions. In A. International (Ed.), ASTM E104-02. West Conshohocken, PA.

Astuti, R. M., Widaningrum, Asiah, N., Setyowati, A., & Fitriawati, R. (2018). Effect of physical modification on granule morphology, pasting behavior, and functional properties of arrowroot (Marantha arundinacea L) starch. *Food Hydrocolloids*, *81*, 23–30.

Atkin, N. J., Abeysekera, R. M., & Robards, A. W. (1998). The events leading to the formation of ghost remnants from the starch granule surface and the contribution of the granule surface to the gelatinization endotherm. *Carbohydrate Polymers*, *36*(2–3), 193–204.

Banchathanakij, R., & Suphantharika, M. (2009). Effect of different β-glucans on the gelatinisation and retrogradation of rice starch. *Food Chemistry*, *114*(1), 5–14.

Biliaderis, C. G. (2009). Structural Transitions and Related Physical Properties of Starch. In *Starch* (pp. 293–372).

Biliaderis, C. G., Page, C. M., Maurice, T. J., & Juliano, B. O. (1986). Thermal Characterization of Rice Starches: A Polymeric Approach to Phase Transitions of Granular Starch. *Journal of Agricultural and Food Chemistry*, *34*(1), 6–14.

Buléon, A., Colonna, P., Planchot, V., & Ball, S. (1998). Starch granules: Structure and biosynthesis. *International Journal of Biological Macromolecules*, Vol. 23, pp. 85–112.

Capron, I., Robert, P., Colonna, P., Brogly, M., & Planchot, V. (2007). Starch in rubbery and glassy states by FTIR spectroscopy. *Carbohydrate Polymers*, *68*(2), 249–259.

Chen, P., Xie, F., Zhao, L., Qiao, Q., & Liu, X. (2017). Effect of acid hydrolysis on the multi-scale structure change of starch with different amylose content. *Food Hydrocolloids*, *69*, 359–368.

Chen, X., Du, X., Chen, P., Guo, L., Xu, Y., & Zhou, X. (2017). Morphologies and gelatinization behaviours of high-amylose maize starches during heat treatment.

Carbohydrate Polymers, *157*, 637–642.

Copeland, L., Blazek, J., Salman, H., & Tang, M. C. (2009). Form and functionality of starch. *Food Hydrocolloids*, *23*(6), 1527–1534.

Ding, L., Zhang, B., Tan, C. P., Fu, X., & Huang, Q. (2019). Effects of limited moisture content and storing temperature on retrogradation of rice starch. *International Journal of Biological Macromolecules*, *137*, 1068–1075.

Dubois, M., Gilles, K. A., Hamilton, J. K., Rebers, P. A., & Smith, F. (1956). Colorimetric method for determination of sugars and related substances. *Analytical Chemistry*, *28*, 350–356.

Eerlingen, R. C., & Delcour, J. A. (1995). Formation, analysis, structure and properties of type III enzyme resistant starch. *Journal of Cereal Science*, *22*(2), 129–138.

Englyst, H., Wiggins, H. S., & Cummings, J. H. (1982). Determination of the non-starch polysaccharides in plant foods by gas - Liquid chromatography of constituent sugars as alditol acetates. *The Analyst*, *107*(1272), 307–318.

Epp, J. (2016). X-Ray Diffraction (XRD) Techniques for Materials Characterization. In *Materials Characterization Using Nondestructive Evaluation (NDE) Methods* (pp. 81–124).

Fonseca-Florido, H. A., Méndez-Montealvo, G., Velazquez, G., & Gómez-Aldapa, C. A. (2016). Thermal study in the interactions of starches blends: Amaranth and achira. *Food Hydrocolloids*, *61*, 640–648.

Fontana, A. J. (2008). Appendix A: Water Activity of Saturated Salt Solutions. In *Water Activity in Foods* (pp. 391–393).

Gallant, D. J., Bouchet, B., & Baldwin, P. M. (1997). Microscopy of starch: Evidence of a new level of granule organization. *Carbohydrate Polymers*, *32*(3–4), 177–191.

García, M. A., Pinotti, A., Martino, M. N., & Zaritzky, N. E. (2004). Characterization of composite hydrocolloid films. *Carbohydrate Polymers*, *56*(3), 339–345.

Goodfellow, B. J., & Wilson, R. H. (1990). A fourier transform IR study of the gelation of amylose and amylopectin. *Biopolymers*, *30*(13–14), 1183–1189.

Guo, P., Yu, J., Copeland, L., Wang, S., & Wang, S. (2018). Mechanisms of starch gelatinization during heating of wheat flour and its effect on in vitro starch digestibility. *Food Hydrocolloids*, *82*, 370–378.

Henning, S., & Adhikari, R. (2017). Scanning Electron Microscopy, ESEM, and X-ray Microanalysis. In *Microscopy Methods in Nanomaterials Characterization* (pp. 1–30).

Hizukuri, S. (1986). Polymodal distribution of the chain lengths of amylopectins, and its significance. *Carbohydrate Research*, *147*(2), 342–347.

Hsu, R. J. C., Lu, S., Chang, Y. H., & Chiang, W. (2015). Effects of added water and retrogradation on starch digestibility of cooked rice flours with different amylose content. *Journal of Cereal Science*, *61*, 1–7.

Hu, X. P., Xie, Y. Y., Jin, Z. Y., Xu, X. M., & Chen, H. Q. (2014). Effect of single-, dual-, and triple-retrogradation treatments on in vitro digestibility and structural characteristics of waxy wheat starch. *Food Chemistry*, *157*, 373–379.

Imberty, A., Buléon, A., Tran, V., & Péerez, S. (1991). Recent Advances in Knowledge of Starch Structure. *Starch - Stärke*, *43*(10), 375–384.

Jagannadham, K., Parimalavalli, R., & Surendra Babu, A. (2017). Effect of triple retrogradation treatment on chickpea resistant starch formation and its characterization. *Journal of Food Science and Technology*, *54*(4), 901–908.

Joye, I. J. (2018). Starch. In *Encyclopedia of Food Chemistry* (pp. 256–264).

Kainuma, K., & French, D. (1971). Nägeli amylodextrin and its relationship to starch granule structure. I. Preparation and properties of amylodextrins from various starch types. *Biopolymers*, *10*(9), 1673–1680.

Kim, M. A., Choi, S. J., & Moon, T. W. (2015). Digestibility of retrograded starches with A- and B-type crystalline structures. *Journal of the Korean Society for Applied Biological Chemistry*, *58*(4), 487–490.

Le Corre, D., Bras, J., & Dufresne, A. (2010). Starch nanoparticles: A review. *Biomacromolecules*, Vol. 11, pp. 1139–1153.

Lian, X., Cheng, K., Wang, D., Zhu, W., & Wang, X. (2018). Analysis of crystals of retrograded starch with sharp X-ray diffraction peaks made by recrystallization of amylose and amylopectin. *International Journal of Food Properties*, *20*, S3224–S3236.

Lin, L., Guo, D., Zhao, L., Zhang, X., Wang, J., Zhang, F., & Wei, C. (2016). Comparative structure of starches from high-amylose maize inbred lines and their hybrids. *Food Hydrocolloids*, *52*, 19–28.

Liu, Y., Yu, J., Copeland, L., Wang, S., & Wang, S. (2019). Gelatinization behavior of starch: Reflecting beyond the endotherm measured by differential scanning calorimetry. *Food Chemistry*, *284*, 53–59.

Lopez-Rubio, A., Flanagan, B. M., Gilbert, E. P., & Gidley, M. J. (2008). A novel approach for calculating starch crystallinity and its correlation with double helix content: A combined XRD and NMR study. *Biopolymers*, *89*(9), 761–768.

Ma, Z., & Boye, J. I. (2018). Research advances on structural characterization of resistant starch and its structure-physiological function relationship: A review. *Critical Reviews in Food Science and Nutrition*, *58*(7), 1059–1083.

Ma, Z., Yin, X., Chang, D., Hu, X., & Boye, J. I. (2018). Long- and short-range structural characteristics of pea starch modified by autoclaving, α-amylolysis, and pullulanase debranching. *International Journal of Biological Macromolecules*, *120*, 650–656.

Matignon, A., & Tecante, A. (2017). Starch retrogradation: From starch components to cereal products. *Food Hydrocolloids*, *68*, 43–52.

Meyer, K. H., Bernfeld, P., Boissonnas, R. A., Gürtler, P., & Noelting, G. (1949). Starch solutions and pastes and their molecular interpretation. *Journal of Physical and Colloid*

Chemistry, *53*(3), 319–334.

Morrison, W. R., Tester, R. F., Gidley, M. J., & Karkalas, J. (1993). Resistance to acid hydrolysis of lipid-complexed amylose and lipid-free amylose in lintnerised waxy and non-waxy barley starches. *Carbohydrate Research*, *245*(2), 289–302.

O'Brien, S., Wang, Y. J., Vervaet, C., & Remon, J. P. (2009). Starch phosphates prepared by reactive extrusion as a sustained release agent. *Carbohydrate Polymers*, *76*(4), 557–566.

Ogunsona, E., Ojogbo, E., & Mekonnen, T. (2018). Advanced material applications of starch and its derivatives. *European Polymer Journal*, Vol. 108, pp. 570–581.

Oostergetel, G. T., & van Bruggen, E. F. J. (1993). The crystalline domains in potato starch granules are arranged in a helical fashion. *Carbohydrate Polymers*, *21*(1), 7–12.

Öztürk, S., & Mutlu, S. (2018). Physicochemical properties, modifications, and applications of resistant starches. In *Starches for Food Application: Chemical, Technological and Health Properties* (pp. 297–332).

Pedrosa Silva Clerici, M. T., Sampaio, U. M., & Schmiele, M. (2018). Identification and analysis of starch. In *Starches for Food Application: Chemical, Technological and Health Properties* (pp. 23–69).

Pérez, S., & Bertoft, E. (2010). The molecular structures of starch components and their contribution to the architecture of starch granules: A comprehensive review. *Starch/ Stärke*, Vol. 62, pp. 389–420.

Peymanpour, G., Marcone, M., Ragaee, S., Tetlow, I., Lane, C. C., Seetharaman, K., & Bertoft, E. (2016). On the molecular structure of the amylopectin fraction isolated from "high-amylose" ae maize starches. *International Journal of Biological Macromolecules*, *91*, 768–777.

Pfister, B., & Zeeman, S. C. (2016). Formation of starch in plant cells. *Cellular and Molecular Life Sciences*, Vol. 73, pp. 2781–2807.

Pratiwi, M., Faridah, D. N., & Lioe, H. N. (2018). Structural changes to starch after acid hydrolysis, debranching, autoclaving-cooling cycles, and heat moisture treatment (HMT): A review. *Starch/Stärke*, Vol. 70.

Pu, H., Chen, L., Li, L., & Li, X. (2013). Multi-scale structural and digestion resistibility changes of high-amylose corn starch after hydrothermal-pressure treatment at different gelatinizing temperatures. *Food Research International*, *53*(1), 456–463.

Rabek, J. F. (1980). *Experimental methods in polymer chemistry: Applications of wide angle X-ray diffraction (WAXD) to the study of the structure of polymers*. Chichester: Wiley Interscience.

Raigond, P., Ezekiel, R., & Raigond, B. (2015). Resistant starch in food: a review. *Journal of the Science of Food and Agriculture*, *95*(10), 1968–1978.

Ratnaningsih, N., Suparmo, Harmayani, E., & Marsono, Y. (2020). Physicochemical properties, in vitro starch digestibility, and estimated glycemic index of resistant starch from cowpea (Vigna unguiculata) starch by autoclaving-cooling cycles. *International*

Journal of Biological Macromolecules, *142*, 191–200.

Robin, J. P., Mercier, C., Charbonn, R., & Guilbot, A. (1974). Lintnerized starches gel-filtration and enzymatic structure of insoluble residues from prolonged acid treatment of potato starch. *Cereal Chemistry*, *51*, 389–406.

Shittu, T. A., Idowu-Adebayo, F., Adedokun, I. I., & Alade, O. (2015). Water vapor adsorption characteristics of starch−albumen powder and rheological behavior of its paste. *Nigerian Food Journal*, *33*(1), 90–96.

Singh, N., Singh, J., Kaur, L., Sodhi, N. S., & Gill, B. S. (2003). Morphological, thermal and rheological properties of starches from different botanical sources. *Food Chemistry*, Vol. 81, pp. 219–231.

Slade, L., & Levine, H. (1993). Water relationships in starch transitions. *Carbohydrate Polymers*, *21*(2–3), 105–131.

Sullivan, W. R., & Small, D. M. (2019). Resistant Starch (RS) in Breads: What It Is and What It Does. In *Flour and Breads and their Fortification in Health and Disease Prevention* (pp. 375–386).

Tacer-Caba, Z., & Nilufer-Erdil, D. (2019). Resistant Starch. *Encyclopedia of Food Chemistry*, 571–575.

Takeda, Y., Shitaozono, T., & Hizukuri, S. (1990). Structures of sub-fractions of corn amylose. *Carbohydrate Research*, *199*(2), 207–214.

Tester, R. F., Karkalas, J., & Qi, X. (2004). Starch—composition, fine structure and architecture. *Journal of Cereal Science*, *39*(2), 151–165.

Tian, Y., Li, Y., Xu, X., & Jin, Z. (2011). Starch retrogradation studied by thermogravimetric analysis (TGA). *Carbohydrate Polymers*, *84*(3), 1165–1168.

Tian, Y., Zhang, L., Xu, X., Xie, Z., Zhao, J., & Jin, Z. (2012). Effect of temperature-cycled retrogradation on slow digestibility of waxy rice starch. *International Journal of Biological Macromolecules*, *51*(5), 1024–1027.

Trinh, K. S. (2015). Recrystallization of starches by hydrothermal treatment: digestibility, structural, and physicochemical properties. *Journal of Food Science and Technology*, *52*(12), 7640–7654.

Utrilla-Coello, R. G., Hernández-Jaimes, C., Carrillo-Navas, H., González, F., Rodríguez, E., Bello-Pérez, L. A., … Alvarez-Ramirez, J. (2014). Acid hydrolysis of native corn starch: Morphology, crystallinity, rheological and thermal properties. *Carbohydrate Polymers*, *103*(1), 596–602.

Valenzuela-Díaz, E. (2019). *Efecto de la hidrólisis ácida en la morfología y en las propiedades funcionales de almidón de maíz* (Tesis de licenciatura). Tecnológico Nacional de México, Instituto Tecnológico de Acapulco, Guerrero, México.

Vamadevan, V., & Bertoft, E. (2015). Structure-function relationships of starch components. *Starch - Stärke*, *67*(1–2), 55–68.

Vamadevan, V., & Bertoft, E. (2018). Impact of different structural types of amylopectin on retrogradation. *Food Hydrocolloids*, *80*, 88–96.

Waigh, T. A., Gidley, M. J., Komanshek, B. U., & Donald, A. M. (2000). The phase transformations in starch during gelatinisation: A liquid crystalline approach. *Carbohydrate Research*, *328*(2), 165–176.

Wang, H., Zhang, B., Chen, L., & Li, X. (2016). Understanding the structure and digestibility of heat-moisture treated starch. *International Journal of Biological Macromolecules*, *88*, 1–8.

Wang, S., Blazek, J., Gilbert, E., & Copeland, L. (2012). New insights on the mechanism of acid degradation of pea starch. *Carbohydrate Polymers*, *87*(3), 1941–1949.

Wang, S., & Copeland, L. (2013). Molecular disassembly of starch granules during gelatinization and its effect on starch digestibility: A review. *Food and Function*, Vol. 4, pp. 1564–1580.

Wang, S., & Copeland, L. (2015). Effect of acid hydrolysis on starch structure and functionality: a review. *Critical Reviews in Food Science and Nutrition*, *55*(8), 1081–1097.

Wang, S., Li, C., Copeland, L., Niu, Q., & Wang, S. (2015). Starch Retrogradation: A Comprehensive Review. *Comprehensive Reviews in Food Science and Food Safety*, *14*(5), 568–585.

Warren, F. J., Gidley, M. J., & Flanagan, B. M. (2016). Infrared spectroscopy as a tool to characterise starch ordered structure - A joint FTIR-ATR, NMR, XRD and DSC study. *Carbohydrate Polymers*, *139*, 35–42.

Xu, J., Ma, Z., Ren, N., Li, X., Liu, L., & Hu, X. (2019). Understanding the multi-scale structural changes in starch and its physicochemical properties during the processing of chickpea, navy bean, and yellow field pea seeds. *Food Chemistry*, *289*, 582–590.

Yang, J., Xie, F., Wen, W., Chen, L., Shang, X., & Liu, P. (2016). Understanding the structural features of high-amylose maize starch through hydrothermal treatment. *International Journal of Biological Macromolecules*, *84*, 268–274.

Yin, X., Ma, Z., Hu, X., Li, X., & Boye, J. I. (2018). Molecular rearrangement of Laird lentil (Lens culinaris Medikus) starch during different processing treatments of the seeds. *Food Hydrocolloids*, *79*, 399–408.

Zhang, B., Selway, N., Shelat, K. J., Dhital, S., Stokes, J. R., & Gidley, M. J. (2017). Tribology of swollen starch granule suspensions from maize and potato. *Carbohydrate Polymers*, *155*, 128–135.

Zhang, H., Hou, H., Liu, P., Wang, W., & Dong, H. (2019). Effects of acid hydrolysis on the physicochemical properties of pea starch and its film forming capacity. *Food Hydrocolloids*, *87*, 173–179.

Zhou, D., Ma, Z., Yin, X., Hu, X., & Boye, J. I. (2019). Structural characteristics and physicochemical properties of field pea starch modified by physical, enzymatic, and

acid treatments. *Food Hydrocolloids*, *93*, 386–394.

Zhou, X., Wang, R., Yoo, S. H., & Lim, S. T. (2011). Water effect on the interaction between amylose and amylopectin during retrogradation. *Carbohydrate Polymers*, *86*(4), 1671–1674.

Zhou, Y., Meng, S., Chen, D., Zhu, X., & Yuan, H. (2014). Structure characterization and hypoglycemic effects of dual modified resistant starch from indica rice starch. *Carbohydrate Polymers*, *103*(1), 81–86.

Zia-ud-Din, Xiong, H., & Fei, P. (2017). Physical and chemical modification of starches: A review. *Critical Reviews in Food Science and Nutrition*, Vol. 57, pp. 2691–2705.